12-2020

Mono and Multi-Objective Optimization and Modeling of Machining Performance in Face Milling of Ti6Al4V Alloy

Al Mazedur Rahman

The University of Texas Rio Grande Valley

MONO AND MULTI-OBJECTIVE OPTIMIZATION AND MODELING OF MACHINING PERFORMANCE IN FACE MILLING OF Ti6Al4V ALLOY

A Thesis

by

AL MAZEDUR RAHMAN

Submitted to the Graduate College of
The University of Texas Rio Grande Valley
In partial fulfillment of the requirements for the degree of

MASTER OF SCIENCE IN ENGINEERING

December 2020

Major Subject: Manufacturing Engineering

MONO AND MULTI-OBJECTIVE OPTIMIZATION AND MODELING OF MACHINING PERFORMANCE IN FACE MILLING OF Ti6Al4V ALLOY

A Thesis
by
AL MAZEDUR RAHMAN

COMMITTEE MEMBERS

Dr. Anil Srivastava
Chair of Committee

Dr. Jianzhi Li
Committee Member

Dr. Rajiv Nambiar
Committee Member

Dr. Kye Hwan (Kevin) Lee
Committee Member

December 2020

ABSTRACT

Rahman, Al Mazedur, Mono and Multi-Objective Optimization and Modeling of Machining Performance in Face Milling of Ti6Al4V Alloy Master of Science in Engineering (MSE), December 2020, 70 pp., 25 Figures, 23 Tables, 111 References.

Titanium alloys are extensively used in numerous industries like aerospace, automotive, military, etc., due to their exclusive characteristics. But machining these alloys has always been challenging for manufacturers. This research investigates the effect of radial depth of cut on cutting forces, tool life, surface roughness (Ra), and material removal rate (MRR) during face milling of Ti6Al4V alloy. It also aims to perform mono and multi-objective optimization of response characteristics to determine the optimal input parameters, namely cutting speed, feed rate, and radial depth of cut. Taguchi method and analysis of variance (ANOVA) have been used for mono-objective optimization, whereas Taguchi-based Grey relational analysis (GRA) and Genetic algorithm (GA) have been used for multi-objective optimization. Regression analysis has been performed for developing mathematical models to predict Ra, tool life, average cutting forces, and MRR. According to ANOVA analysis, the most significant parameter for tool life is cutting speed. For MRR and average cutting force (Avg. F_Y), the most influential parameter is the radial depth of cut. On the other hand, feed rate is the most significant parameter for Ra and average feed force (Avg. F_X). The optimal combination of input parameters for tool life and Avg. F_Y is 50 m/min cutting speed, 0.2 mm/rev feed rate, and 7.5 mm radial depth of cut. However,

the optimal parameters for Ra are 65 m/min cutting speed, 0.2 mm/rev feed rate, and 7.5 mm radial depth of cut. For Avg. F_X, the optimal conditions are 57.5 m/min cutting speed, 0.2 mm/rev feed rate, and 7.5 mm radial depth of cut. Similarly, for MRR, the optimal parameters are 65 m/min cutting speed, 0.3 mm/rev feed rate, and 12.5 mm radial depth of cut. A validation experiment has been conducted at the optimal Ra parameters, which shows an improvement of 31.29% compared to the Ra measured at the initial condition. A minor error has been found while comparing the experimental data with the predicted values calculated from the mathematical models. GRA for multi-objective (3 objectives: tool life, Ra, and Avg. F_Y) optimization has improved 55.81% tool life, 6.12% Ra, and 23.98% Avg. F_Y. ANOVA analysis based on grey relational grade has demonstrated that radial depth of cut is the most significant parameter for multi-objective (three objectives) optimization during the face milling of Ti6Al4V. The results obtained from the GRA considering four output characteristics (tool life, Ra, Avg. F_Y, and MRR) are compared with GA optimization results for both roughing and finishing, and a negligible deviation has been observed.

DEDICATION

I dedicate my work to my mother, Shahida Khatun; my father, Md. Siddiqur Rahman; and my sister Mayeda Rahman Prome. Thanks to the almighty for helping me and guiding me through the difficult times. Without the constant support and help of my supervisor, family, and friends, my journey here at UTRGV would not have been possible.

ACKNOWLEDGEMENT

I would like to acknowledge my supervisor, Dr. Anil K. Srivastava, for his outstanding guidance and support. His knowledge and expertise in the advanced machining field and his ongoing mentorship have helped me overcome all the difficulties I faced during this master's program. I am delighted that I got the opportunity to work in the Advanced Machining Lab under his supervision. Besides, I am very thankful to my colleagues S M Abdur Rob, and Edgar Turribiates. I would specially mention S M Abdur Rob as his continuous learning mentality, and industriousness motivated me a lot. I have learned a lot from Edgar Turrubiates, as he has excellent experience in CNC machining. I want to thank Prosanto Biswas, Abu Musa Abdullah Sourav, and Aminur Rashid Chowdhury for making my journey smooth at the earlier stage. I am also thankful to Hasan Anwar Niloy, Abdullah Al Masum, Apu Deb, Mostafa Meraj Pasha, Taeba Tuba, Saumik Sakib, Shofe Ahmed Mazumder, Sadia Sharmin, Md. Fazle Rabby, Mohammad Salman, Fatema Hamim, Sadaf, Hamanti, Wasif Zaman Jitu, Afsana Akter Moushumi, Mirza Aditto Billah (Panda), Al Amin, and Tushar Abdullah Fatta for their continuous encouragement and support.

TABLE OF CONTENTS

LIST OF TABLES

LIST OF FIGURES

Page

CHAPTER I

INTRODUCTION

Titanium and its alloys have extraordinary properties like extreme corrosion and fracture resistance, high strength-to-density ratio, and show unique performance at elevated temperatures. These alloys are about 40% lighter and nearly possess similar mechanical and physical properties as steel. Due to these capabilities, titanium alloys are extensively used in aircraft engines, airframe manufacturers, and military applications to decrease the weight and enhance durability in extreme circumstances for increasing mobility and battle efficiency [1]. Usually, for alloying with titanium, materials such as V, Al, Mn, Sn, Zr, Mo, S, etc., are used [2]. Many alloys like Ti6Al4V, Ti6Al2Sn4Zr2Mo, Ti5Al2.5Sn, etc., are produced by combining these materials. Ti6Al2Sn4Zr2Mo is used mostly in discs, blades, jet engines; Ti6Al4V is used in jet engines, gas turbines, airframe components, and Ti5Al2.5Sn is used in a corrosive environment, gas turbine engines, aerospace structures [3]. Among all the alloys, Ti6Al4V is the most popular one and occupies most of the market percentage of titanium products used all over the world now [4]. The high strength-to-weight ratio, biocompatibility, high corrosion resistance properties have extended its use in bridges and implants, marine, automobile, energy, chemical, and biomedical industries [4-8]. Titanium alloys are divided into three main groups which are α-alloys, β-alloys, and α/β-alloys and Ti6Al4V belongs to α/β-alloys, which has a chemical composition of 6% Aluminum, 4% Vanadium, .25% Iron, .2% Oxygen, and the rest is Titanium [9].

Although having many superior qualities, it is one of the most difficult-to-cut materials. Titanium alloys are hard to machine because of their high chemical reactivity at high temperatures, comparatively low modulus of elasticity, high strength, low heat conductivity, high rigidity [10, 11]. These characteristics of Ti6Al4V cause severe manufacturing difficulties, which makes the machining process costly. Typically, manufacturers make the components by forging or casting to the nearest final shape in military applications, then milling with roughing and final cut results in the finished product [12].

While machining titanium, no built-up edge forms on the cutting tool, which enhances the abrading and alloying action of the thin chip forcing over a small tool chip contact area under high pressure [13]. This high pressure along with less heat conductivity creates a high temperature in the tooltip area. As the material shows a hot strength behavior, it offers the highest pulsating loads because of the formation of segmented chips [14], resulting in high-pressure loads through the reduced contact surface. High thermal stress grows at the cutting edge due to low heat dissipation by the chips and workpiece. While machining steels and aluminum alloys, a large amount of the heat generated is transmitted into the chips. But, when it comes to titanium alloys, a significant portion of the heat gets transferred into the cutting tool, which makes a high heat concentration on the tool's cutting edge, resulting in a faster tool failure [15]. Low thermal conductivity and high thermal capacity are the main reason for absorbing 30% more heat by the cutting edge compared to steel machining [16]. Enhanced diffusion and adhesion processes are observed where thermal stress emerges. Self-induced chatter and cutting forces are reasons for continuous tool chippings and, finally, tool failure. Due to the low Young's modulus, there is a vibration affinity of unstable workpieces. As heat is accumulated in the cutting zone, a strong affinity to adhesion is observed. Titanium chips can make a hazard of exoergic reaction with atmospheric oxygen [17-19]. For these reasons, while machining titanium alloys, the parameters are restricted to avoid the heat build-up edge formation.

In selecting cutting tool material, high-speed steel (HSS) tools can be used for full-cut operations for their high tenacity [20]. Tungsten carbide/Cobalt (WC/Co) has superiority in all cutting applications of titanium alloys, no matter what wear mechanism occurs [21]. U.S. industry grade C2, represented by International organization for standardization (ISO) code K20 (Carbide tools having a PVD coating of TiAlN) has been found to be the best grade of cutting tool in machining applications for titanium alloys [22]. Research indicates that K grade carbides like WC/Co alloys with Co percentage of 6 wt% and medium grain size can give the optimum performance for machining titanium alloys [23]. Straight Cobalt-base tungsten carbide implanted with Chlorine and Indium is also proven efficient in cutting titanium and its alloys [24]. P grades of ISO codes used for steel cutting are not efficient for cutting titanium alloys as they have mixed grain sizes and inauspicious thermal properties [25, 26]. All the cemented carbide tools coated with TiCN, TiC, TiN, Al_2O_3-TiC, TiC-TiN, HfN, TiB_2 have been tested and showed larger wear rates than straight grade cemented carbides [27, 28]. The coating of TiN with the PVD technique has given an excellent performance while milling titanium alloys [29]. HSS tools like M1, M2, M7, M10 grades have shown promising results while machining titanium alloys, but M33, M40, M42 grades are the best to use [30].

The research field related to cutting fluid, in general, is quite inconsistent as some researchers have used dry cutting, and some researchers tried conventional flood cooling [31]. In some cases, metalworking fluid plays a vital role in increasing the tool life and machining quality. At lower speed, coolant can contribute a significant impact as it can improve average heat extraction from cutting zone, alter viscosity, surface tension, etc. Lubrication with a 3-7% percentage is generally used in cutting titanium alloys [32, 33]. The cost of cutting fluid is about 15-17% of the total production cost, whereas cutting tools are accounted for only 2-4% of the total cost [34]. Environment-friendly cutting fluids, minimum quantity lubrication (MQL), dry cutting, biodegradable vegetable oil, and many investigations are going on for machining of titanium alloys at less cost and in a more effective way [35, 36]. The variation in the efficacy of cutting fluid and the cooling method impacts machining of titanium alloy significantly [37]. The lubrication method's actual problem is that the coolant fails to reach the real cutting edge because the extreme heat developed in the tool-workpiece-chip interface evaporates the coolant at a higher cutting speed. The MQL method reduces the production cost and improves Ra. This method is called the near dry lubrication method or micro lubrication method, where cutting fluid used for machining is much lower than the flood cooling method [38]. In some recent articles, a new cooling method has been shown where an atomized-based cutting fluid spray system has been introduced [39].

As there are many difficulties in the machinability of titanium alloys, many researchers have used different modeling and optimization techniques. Response surface methodology (RSM) has been used to model cutting-forces data obtained from machining Ti6Al4V by physical vapor deposition (PVD) coated tools [40]. Various cutting tools with different coatings have been used in an article for machining Ti6Al4V, where the Taguchi technique has been used for analyzing the data [15].

Ra is considered as one of the most important quality characteristics for determining the surface quality. Better Ra facilitates improvements in various characteristics such as corrosion and wear resistance, fatigue strength, friction, etc. To minimize the production cost, manufacturers focus on increasing tool life or reducing tool wear. Tool wear has a significant effect on cutting forces, which plays a crucial role in measuring power consumption and designing the cutting tool [41]. MRR is directly related to production time. Therefore, tool life, cutting forces, Ra, and MRR have been considered for optimization as the performance characteristics in this study. All those output characteristics have a relation with the cutting parameters. Machining operators use a trial and error basis determination process as the theoretical calculation is challenging [42]. These processes can be lengthy and repetitive, and empirical, which results in inefficiency. For improving yield in the industrial environment, the Taguchi process has been introduced. It can consider multiple factors at once and show the insensitive factors resulting in greater output in the manufacturing process and improve the final product's performance.

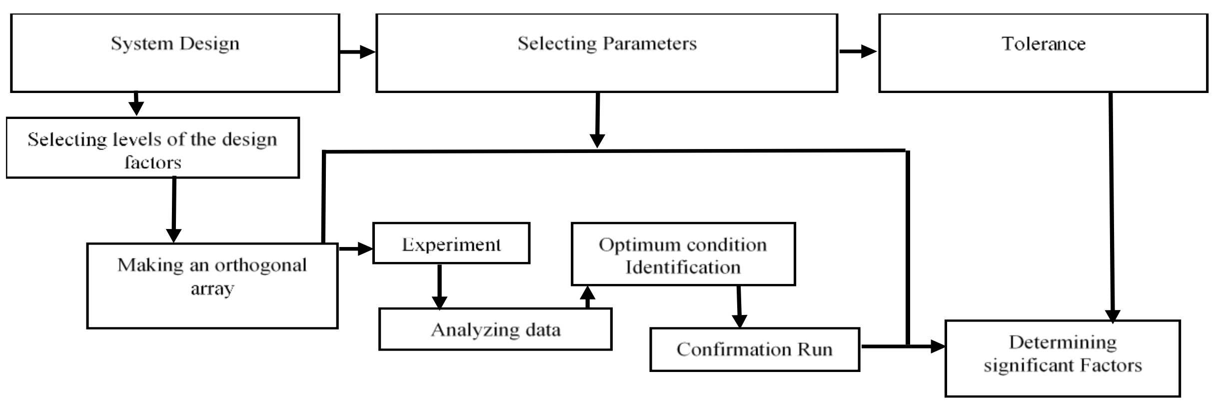

Figure 1. Taguchi Design System

Taguchi analysis shortens the product development cycle for design and production, which decreases cost and increases profit. From Figure 1, Taguchi design can be better understood. The whole designing system is divided into three steps, where parameter design is the most significant step [43]. The factors that affect the outputs are required for making the orthogonal array, and then experiments are conducted according to the orthogonal array. The goal is to obtain the best output characteristics by analyzing the experimental data obtained and then conducting the validation experiment at the optimal parameters.

For applying Taguchi design, factors that affect the output characteristics should be identified at first from the literature. The most important factors related to tool wear, Ra, forces, and MRR are found in the literature. Factors that affect those output characteristics are mainly speed, feed, depth of cut, cutter runout, cutter geometry, tool wear, vibration, forces, etc. [44]. Another article added tool nose radius, flank wear as control factors [45]. One research stated that cutting speed, feed per tooth, and cutting depth(only axial depth of cut) can be considered as control parameters for finding optimum surface integrity and cutting force [46]. Multiple characteristics can be studied with these factors, such as material removed, burr height in face milling operation. Most of the articles show the use of three factors in face milling: speed, feed, and axial depth of cut. These articles proved that the Taguchi design worked very well in optimizing all the cutting parameters. Different optimization techniques have been used by researchers along with artificial neural network (ANN) [3].

This study is based on the following five steps.

1. The cutting tool used in this study has a special coating, which is identified with X-ray photoelectron spectroscopy (XPS) and X-Ray Diffraction (XRD) analysis.

2. For Taguchi analysis, the factors usually selected are speed, feed rate, and axial depth of cut. But for this study, radial depth of cut is used in place of the axial depth of cut to see the impact of radial depth of cut on the output characteristics.

3. Analyzing the coated cutting tool's performance and optimizing the parameters for better Ra, increased tool life, reduced forces, and maximum MRR using Taguchi and ANOVA analysis.
4. Regression analysis is performed to predict the output characteristics and a validation experiment is conducted to validate the mathematical models and optimized results.
5. Mono and multi-objective optimization is performed using GRA and GA, and results are compared.

CHAPTER II

LITERATURE REVIEW

In the aerospace industry, machining of titanium alloys is common. Researchers have done extensive work to enhance productivity while machining such high strength alloys. However, machinability and optimization problems are still under investigation to some extent. New cutting tools are developed with different coatings and coating techniques and cutting tool parameters are being optimized depending on various factors. This chapter introduces a concise overview of the face milling of Ti6Al4V and optimization of the different machining process parameters to enhance product quality and productivity.

Previous work on the machining of titanium alloys

Titanium and its alloys have low thermal conductivity; thus, the heat generated by the cutting actions doesn't dissipate rapidly and remains concentrated near the cutting edge. This heat affects the cutting tool life adversely.

Titanium alloys have a high ratio of yield stress to tensile strength (>0.9), and the flow stresses increase rapidly with a strain rate greater than 10^3 s-1 [47]. Strain hardening is extremely influenced by twin dislocation interactions during plastic deformation of titanium alloys [48]. Titanium also shows a high affinity at high temperatures with the cutting tool materials which causes welding of workpiece material to the cutting tool while cutting. Continuous galling, chipping, and smearing on the machined surface result in a fast decrease in tool life. High chemical reactivity, high thermal strength, low thermal conductivity, low modulus of elasticity, high strain hardening, inferior dislocation motion are the main reasons that cause poor machinability of titanium alloys [49].

For process optimization, predictive modeling is the primary step. Finding the relationship between the input parameters, which are independent variables, and output parameters, which are dependent variables, is the main target of predictive modeling. Two approaches are well known to acquire this model: (i) the fundamental practice using analytical systems and (ii) empirical methods. Design of experiments, curve fitting, and many more sophisticated study tools are needed for finding the empirical solution from the obtained experimental data. Considering too many factors in machining of titanium alloys makes it difficult to explain the process, and results obtained are different for each change in phenomenon [50].

Several researchers have used theoretical or fundamental approach. This approach consists of geometric, analytical, or mechanistic modeling methods. This chapter summarizes the findings from various researchers for measuring machining performances while machining different alloys with a focus on titanium alloys.

Cutting Forces/Power

In 1932, researchers started investigating the empirical modeling approach where the equation for cutting forces was presented as a function of feed, depth of cut, and tool wear. Cutting fluid was also considered during the investigations. Comparisons were made between up and down milling for aluminum alloys. That’s where the idea was generated for creating mathematical models for titanium alloys [51]. Analytical models for orthogonal and oblique cutting started developing for the mechanism of metal cutting[52].

For predicting cutting forces, mechanistic models have become popular as these models could predict cutting forces from the theoretical equations having basic machining parameters. These mechanistic models became the basis for deriving empirical equations using based on the experiments and using the exponents or considering the coefficients [53]. Different coefficients were investigated for variety of other materials to make different equations, and several combinations of parameters were tried [54]. While developing models for force predictions, sometimes the cutter geometry was considered an important factor. One of the research groups divided the cutter into different layers and then calculated each layer separately [55]. Many researchers have used this concept.

During milling operations, the tool geometry was defined as a function of number of flutes, cutter's angular position, and flutes' helix angle for discretizing the cutting edge. This theory was only for the tools having constant helix angle and identical profile for all the flutes. For complex shapes, the model didn’t work because the profile was described by combining a cylindrical surface and a semi-spherical surface for the ball end mill. This model limited the geometry into a perfect ball shape geometry as the flutes earlier [56]. Researchers then described the intricate shapes in different geometries and angles, and many limiting functions were obtained while developing the mechanistic models for those complex shapes [57-59].

One researcher presented a model and compared the chip formation for up and down milling for two forces: tangential and normal [60]. Another mechanistic model was proposed by a researcher who represented the dynamics of cutting forces in end milling with variable adaptive control [61].

Another model was described using orthogonal cutting data for three-dimensional cutting for a single point machining tool for predicting forces in plain milling [62]. This model replaced the oblique angle's inclination with the helix angle and worked well for small helix angles. In another research work, for the corner-milling process which is a particular case of peripheral milling, three-dimensional cutting was considered as a collection of orthogonal cuts, and a model was developed based on chip formation and cutting conditions [63]Another researcher used cutting conditions, tool geometry, process and workpiece geometry for the empirical model for face milling [63]. Later, another model was proposed considering the effects of varying chip thickness by applying the theory of orthogonal machining [64]. Both models investigated the orthogonal machining theory for a single cutting tooth. Later, a new model was proposed for multiple-tooth oblique cutting where the process was described for static and dynamic cutting forces in face milling, considering the initial positioning error and eccentricity of the spindle [65]. In another research, the effect of edge-wear was also included in the process modeling [66].

In 1999, a theoretical model was developed based on oblique cutting and mechanics of face milling for predicting cutting forces where the intermittent cutting force and effect of tool wear on chip-load variation were taken into consideration [67]. Later, a different model was proposed where Oxley’s predictive machining theory was applied, and a dynamic shear length model replaced the conventional simplified shear plane model [68]. The prediction modeling of forces can be used for determining one or more performance measures too. The following paragraph elaborates on the use of force modeling for tool-wear and tool failure analysis.

By investigating the cutting tool's breakage in milling, it was shown that tool failure could be determined by first and second-order differentiation of a time-averaged resultant force [69]. A different approach was then taken for on-line monitoring of flank wear, which was based on the variation pattern of cutting force concerning flank wear [70]. The observations found that the radial depth of cut should be considered for the modeling approach. This research emphasizes finding the mathematical equation for force as a function of speed, feed, and radial depth of cut.

Surface Roughness

Analytical methods were used for finding the effect of clearance angle, rake angle, radial chip thickness, the curvature of the tool path, over the quality of surface generated during milling. In the beginning, most of the researches were based on the force modeling approach and then the surface error modeling was predicted by combining the force model, deflection of the end mill, and the radial depth of cut. The researchers found that milling cutter tool path was the most crucial factor at the beginning of this modeling approach for Ra [60].

In another research, cutting forces and surface error prediction models were approached in end milling by considering it as a flexible system, and this model considered the deflection effect on chip-load for finding the balance of cutting forces. This research demonstrated that the deflection of the system reduces the impact of runout along with peak cutting force and maximum surface error [71]. Another researcher added tool dynamics and tool-wear into consideration for predicting Ra [72].

Later, a mathematical model was developed in face milling for Ra, which considered static characteristics of the process such as cutting tool geometry, machining conditions, insert runout, and dynamic characteristics like force and vibration of the process [73]. The chatter vibration was not included in that model, but relative displacement between the workpiece and cutting tool on the cutting process was considered. This model successfully predicted Ra for different feed rates. A dynamic Ra model was also introduced, and bisection method was used to obtain an optimal feed rate.

One empirical model included residual stresses, nose radius, and flank width for predicting surface roughness. Response Surface Methodology (RSM) was used to find the empirical constants, and a second-order equation was used to show dimensional anomalies [45]. Later, the same researcher showed that Ra accuracy was mostly dependent on the value of workpiece hardness and cutting conditions [74].

Classification of various modeling approaches is found in reference [50]. Recently, artificial intelligence tools like GA, neural networks, neuro-fuzzy techniques, programming, and regression-based modeling have also been used to predict Ra [75-78].

For creating the design of experiment, many methods like Box-Behnken design, Taguchi design, factorial design, etc., have been used. RSM was one of the most popular approaches for measuring surface integrity [79]. RSM analyzes the experimental data to create mathematical models for predicting the Ra [80]. But these techniques for the modeling approach had some significant limitations like they couldn’t determine the roughness for various materials [50].

Another approach, called ANOVA analysis, has become much famous for regression analysis, where experimental data are given as input, and by regression analysis, the model is obtained. [81].

In this research, average Ra has been measured using a profilometer. Regression analysis has been performed on those data for obtaining the mathematical model and each input parameter's significance has been calculated using ANOVA analysis. The predicted and experimental values are shown in graph for better understanding in a later chapter. For future work, Adaptive Neuro-Fuzzy Inference system can be developed for predicting Ra and then the results can be compared with conventional analysis results [82, 83].

Tool Life

Better tool life is one of the industry's essential requirements, and many mathematical models have been developed for predicting tool life. Though different approaches have been considered, none of the methods estimates the tool life accurately. Most of the models are for flat-faced tools, in which cases both flank wear and crater wear were considered. The most used tool wear modeling approaches are summarized later in this section.

It was found in 1907 that cutting tool life has a massive impact on the economic success of the cutting or machining industry [84]. High and low cutting speed both were not desirable because the high speed would result in frequent tool changing, and the lower cutting would give less output. The first tool life empirical equation was developed by Taylor as:

$$VT^{n}=\text{C} \tag{2.1}$$

Where V is the machining speed, C is a constant, which represents the cutting speed of one-minute tool life, n is the slope of the curve obtained. The equation was then modified as n varies with different cutting conditions, and many extensions were added after that [85].

$$n = tan\alpha = (logV_1 - logv_2)/(logT_2 - logT_1) \tag{2.2}$$

$$T = KV^{\frac{1}{n}} * f^{\frac{1}{n_1}} * d^{\frac{1}{n_2}} \tag{2.3}$$

Here, f is feed rate, d is depth of cut, V is cutting speed, and n, n_1, n_2, k are constants, and generally n < n_1 < n_2. It means the cutting speed has the most significant impact on tool life and depth of cut has the least impact. In further research, the Brinell hardness number was considered [86].

$$K = VT^{n} * f^{n_1} * d^{n_2} * B * h * n^{1.25} \tag{2.4}$$

Here, n, n_1, n_2 are experimental constants. Then cutting tool geometry was added to the modeling equation [87]. After that, the tool coatings and chip grove geometry were added to the modeling equation [88].

$$T = T_R * W_g * \left(\frac{V_R}{V}\right)^{\frac{W_c}{n}} \tag{2.5}$$

T represents tool life, V is speed, n is from the earlier equation, W_C= effect of tool coating factor and W_g = chip-groove effect factor, T_R is reference tool life, and V_R is reference cutting speed.

$$W_c = \frac{n}{n_c} \tag{2.6}$$

$$W_g = (K * m)/(f^{n_1} * d^{n_2}) \tag{2.7}$$

Here, m is the machining factor.

In one research, a mechanistic modeling approach was taken considering the force equilibrium equation, where the flank force was used as an input, and the effects were calculated for predicting tool life [89]. A similar modeling approach was taken by another researcher considering the uniform tool wear to calculate the constants for speed, feed, and depth of cut [90].

Mono and Multi-objective Optimization process

Some researchers optimized the process parameters (cutting speed, feed rate, and axial depth of cut) for better Ra, minimizing the tool wear, and tool vibration during the face milling of Ti6Al4V alloy using an uncoated carbide insert using the RSM approach [91]. Later, researchers performed mono-objective optimization of cutting forces and Ra by varying three cutting parameters as input factors (cutting speed, feed rate, and axial depth of cut) using ANOVA and Taguchi method, where they observed that the axial depth of cut and feed per tooth were the most significant input parameters for cutting forces and Ra respectively during end-milling of Ti6Al4V alloy [92]. Another research group studied the effects of cutting parameters (cutting speed, feed rate, and axial depth of cut) on tool life, Ra, and MRR by using Taguchi and ANOVA analysis and found that feed rate was the most significant among the cutting parameters in multi-objective optimization [93]. By applying the Taguchi method and ANOVA analysis, a team of researchers investigated the impact of input parameters, namely, cutting speed, feed rate, and axial depth of cut on output characteristics (tool wear, Ra, and cutting forces) during micro-milling of Ti6Al4V alloy and developed corresponding mathematical models by regression analysis to predict the performance characteristics [94].

Mono-objective optimization is widely used for optimizing various response characteristics. But this process cannot find the optimized combination of cutting parameters that can simultaneously improve the multiple output characteristics. Literature survey reveals that different multi-objective optimization techniques such as GRA, GA, etc. have been used in the past to solve this problem. Recently, GRA has been used as a popular statistical tool to optimize complex multi-objective machining systems. Deng developed GRA to find the correlation between input parameters and output characteristics using Grey Relational Grade [95]. For investigating the micro-milling process of Ti6Al4V alloy, one research group used GRA for optimizing the multiple quality characteristics (Ra and burr width) based on the variation of cutting parameters [96]. Another literature search revealed that the researchers performed the multi-objective optimization of Ra, surface microhardness, and surface residual stress by using the GRA method for different cutting parameters during high-speed milling of titanium alloy TB17 [97]. For optimizing both mono and multi-response characteristics of milling AISI 1050 Steel, researchers used Taguchi and GRA, where the axial depth of cut, feed rate, cutting speed, and the number of inserts were used as input parameters [98].

The literature survey reveals that, for multi-objective optimization (tool life, Ra, and Avg. FY) for the face milling of Ti6Al4V alloy, GRA has not been used earlier. In most of the research work, the optimization of the performance characteristics is based on the variation of cutting speed, feed rate, and axial depth of cut. However, the radial depth of cut can also be a significant factor in the milling of Ti6Al4V alloy [99]. In order to investigate the impact of radial depth of cut on cutting force, Ra, tool life, and MRR during face milling of Ti6Al4V alloy, ANOVA and Taguchi analysis have been applied in this study for mono-objective optimization. Also, GRA and GA have been used for performing multi-objective (tool life, Ra, Avg. FY, MRR) optimization. Moreover, mathematical models for tool life, Ra, cutting forces (Avg. FX, Avg. FY), and MRR have been developed through regression analysis to predict the corresponding response characteristics.

CHAPTER III

OBJECTIVES

This research aims to investigate the relationship between cutting parameters (speed, feed rate, and radial depth of cut) and response characteristics (surface roughness (Ra), cutting forces, tool life, and MRR) in face milling of Ti6Al4V. the research is focused on:

- Finding the impact of radial depth of cut on the output characteristics while face milling with coated carbide cutting tools.
- Analyzing the coated cutting tool's performance and conducting mono-objective optimization to obtain better Ra, increased tool life, reduced forces, and increased MRR using Taguchi analysis and determining each parameter's significance on the output characteristics using ANOVA analysis.
- Creating mathematical models by performing regression analysis after analyzing the data as no models are found for predicting output characteristics as a function of cutting speed, feed rate, and radial depth of cut and, subsequently, validation of the mathematical models.
- Performing multi-objective optimization for three and four objectives by using GRA and GA and, finally, comparing the results.

Methodology

Coated cutting tool

The cutting tool is a tungsten carbide coated insert having a specification as SEAN1203AFTN-M14-k, 150. The dimensions of the cutting tool are shown in Figure 2.

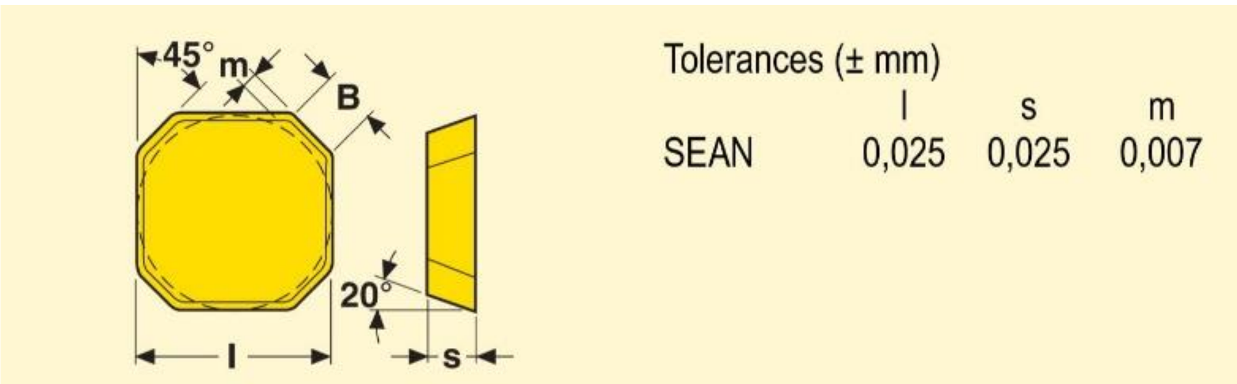

Figure 2. Dimensions of the cutting tool [100]

To analyze the PVD coating on the substrate of the carbide inserts XPS and XRD analysis have been done. The data obtained from the XPS analysis is given below in Table 1.

Table 1. XPS analysis results

Name	Start BE	Peak BE	End BE	Height CPS	FWHM eV	Area (P) CPS. eV	Atomic %
C	294.58	287.87	277.08	313334.4	2.91	1096577	80.91
O	541.08	534.91	525.08	114862.2	3.28	447571.6	13.67
Al	360.08	350.4	343.08	23874.72	3.01	121744.2	1.57
Ti	469.08	458.49	454.08	12501.94	5.15	80592.63	1.03
N	405.58	398.85	395.08	7720.47	4.12	48925.25	2.32
S	174.08	171.02	164.58	3038.78	4.04	13657.27	0.5

As it is a carbide tool, the analysis shows about 81% carbon under the coating. The coating material has been ensured by the XRD analysis given in Figure 3.

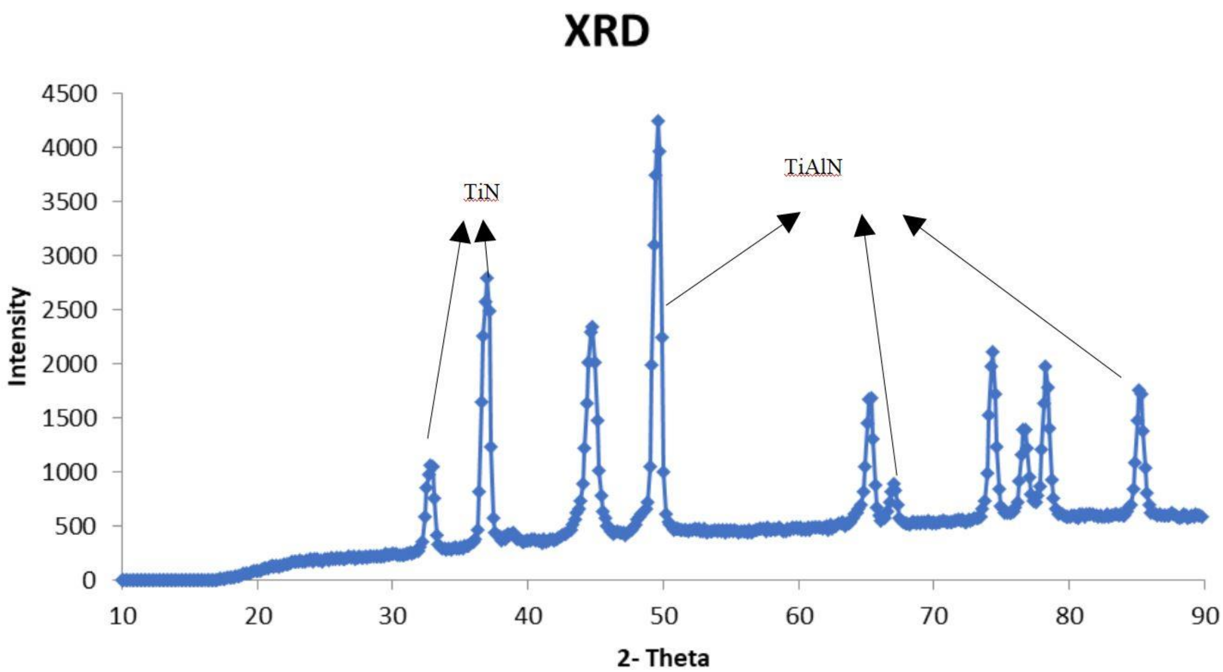

Figure 3. The graph shows the presence of coating materials

TiN coating has the maximum adhesion and ductility characteristics among any of the coatings and has a lower coefficient of friction, good thermal stability, and high wear resistance. These all together reduce built-up edge and give longer tool life if used as a coating [101]. TiAlN coating is suitable for having high hot hardness compared to other coatings. As a result, the coating works better in high-speed dry cutting operations [102].

Taguchi Methodology

Taguchi method uses an orthogonal array to design the experiments and determines the optimal level of input parameters considering their respective ranges. Thus, Taguchi's experimental design is used to organize experiments with a reduced number of experiments. The output characteristics are classified into (i) desirable and (ii) undesirable effects. Desirable effects of output characteristics are known as “Signal” and the undesirable effects are called “Noise”. There are three types of performance characteristics in the analysis of the Signal to Noise (S/N) ratio, which are known as smaller the better, higher the better, and nominal the better. S/N ratio is used to find out the optimal condition of the control parameters. In this experiment, the goal is to minimize the Ra, and the cutting forces and to maximize the tool life, and MRR; therefore, the smaller the better S/N ratio has been applied for Ra, and cutting forces and the larger the better S/N ratio has been applied for tool life, and MRR. The smaller the better S/N ratio is calculated as follows-

$$\mathrm{S/N} = -10\log_{10}\left[\frac{1}{\mathrm{n}}\left(\sum_{\mathrm{i}=1}^{\mathrm{n}} \mathrm{y}_{\mathrm{i}}^{2}\right)\right] \tag{3. 1}$$

The larger the better S/N ratio is calculated as follows-

$$S/N = -10\log_{10}\left[\frac{1}{n}\left(\sum_{i=1}^{n} \frac{1}{y_i^2}\right)\right] \tag{3. 2}$$

Here, y_i is the i^{th} measurement value in a run and n is the number of measurements in each trial. The optimal level of process parameters always corresponds to the highest S/N ratio when the optimization is performed based on a single performance characteristic. However, the optimization of multiple performance characteristics differs from that of single performance characteristic. The higher S/N ratio for one response characteristic may correspond to the lower S/N ratio for another response characteristic. Therefore, the optimization of multiple performance characteristics may require the overall evaluation of the S/N ratio. A GRA has been performed in this study to overcome this problem.

Grey Relational Analysis for multi-objective optimization

In this study, GRA has been used to analyze multiple response characteristics. Normalizing the experimental results of tool life, Avg. F_Y, and Ra is the first step of GRA. The normalized data is used to calculate the grey relational coefficients which demonstrate the correlation between expected and experimental data. In the following step, the grey relational grade is determined using the average value of the grey relational coefficients corresponding to each response characteristic. The calculated grey relational grade is used to evaluate the overall multiple output characteristics. The level of process parameters having the highest grey relational grade is considered as the optimal level. In this way, the GRA transforms the complex multi-objective optimization problem into a single grey relational grade optimization problem [103].

In this study, the higher the better S/N ratio characteristic is used to maximize the tool life, which is expressed as-

$$x_i(k) = \frac{y_i(k) - \min y_i(k)}{\max y_i(k) - \min y_i(k)} \tag{3. 3}$$

The smaller the better S/N ratio characteristic is used to minimize the Avg. F_Y, and Ra, which is expressed as-

$$x_i(k) = \frac{\max y_i(k) - y_i(k)}{\max y_i(k) - mini\ y_i(k)} \tag{3. 4}$$

Here, $x_i(k)$ depicts the value after the grey relational generation, the lowest value of $y_i(k)$ for the *k*th response is $\min y_i(k)$ and the highest value of $y_i(k)$ for the *k*th response is $\max y_i(k)$.

An ideal order x_o (k) (k=1,2, 3) is considered for cutting force, tool life, and Ra. The purpose of grey relational grade is to demonstrate the relational degree among the nine sequences $[x_0(k)\ and\ x_i(k), i = 1,2,3,\dots,9; k = 1,2,3]$. The grey relational coefficient, $\phi_i(k)$ is calculated as follows,

$$\phi_i(k) = \frac{\delta_{min} + \zeta\delta_{max}}{\delta_{0i}(k) + \zeta\delta_{max}} \tag{3. 5}$$

Where, $\delta_{0i} = \|x_0(k) - x_i(k)\|$ = difference of absolute value between $x_0(k)$ and $x_i(k)$; ζ= distinguishing coefficient (0~1); $\delta_{min} = \forall j^{min} \in i\forall k^{min}\|x_0(k) - xj(k)\|$ = smallest value of δ_{0i}; and $\delta_{max} = \forall j^{max} \in i\forall k^{max}\|x_0(k) - xj(k)\|$ = largest value of δ_{0i}. Using the average value of the grey relational coefficients, the grey relational grade ψ_i can be calculated from the following equation.

$$\psi_i = \frac{1}{n}\sum_{k=1}^{n}\phi_i(k) \tag{3. 6}$$

Here, n indicates the number of process outputs. The higher value of the grey relational grade indicates not only a stronger relational degree between the reference sequence $x_0(k)$ and the given sequence $x_i(k)$ but also the optimality of the corresponding cutting parameter [104].

In this study, Analysis of Variance (ANOVA) has been performed along with GRA to predict the optimal combination of process parameters. GRA has been used for optimizing three objectives (tool life, Ra, Avg. F_Y) and four objectives (tool life, Ra, Avg. F_Y, and MRR) separately.

Regression Analysis

Regression analysis is used as a statistical tool for developing a model to find out the relationship between the dependent and independent variables. Generally, the first-order modeling form is expressed as follows-

$$y = \beta_0 + \sum_{i=1}^{k} \beta_i x_i + \varepsilon \tag{3. 7}$$

Here, β, k, and ε represent the coefficient of each term, number of independent variables, and an error respectively.

The value of the correlation coefficient (R^2) is used to justify the validity of the obtained first-order model. Higher R^2 indicates that the relationship between the face milling parameters and the response values is high.

ANOVA analysis

ANOVA analysis is used to identify the significant machining parameters that influence the output characteristic. In this analysis, the total variation of each input parameter is divided into proper elements. By using equation (3. 8) the total sum of squares can be calculated,

$$SS_T = \sum y_i^2 \tag{3. 8}$$

For i =1, 2, …., n. This can also be expressed as

$$SS_T = SS_m + SS_e \tag{3. 9}$$

Here, mean of sum squares $SS_m = nM^2$ and error sum of squares $SS_e = \sum (y_i - M)^2$ where $M = \frac{\sum y_i}{n}$ $(i = 1,2 \dots n)$.

While performing ANOVA for GRA, the total variation of the grey relational grades is calculated using the sum of the squared deviations from the total mean of the grey relational grade. Then the contribution of each machining parameter and the error is calculated. The total sum of the squared deviations SS_T is calculated from the total mean of the grey relational grade ψ_m using the following equation-

$$SS_T = \sum_{j=1}^{p} \left(\psi_j - \psi_m\right)^2 \tag{3.10}$$

Where, p= number of experiments in the orthogonal array, and ψ_j= mean of the grey the relational grade for the j^{th} experiment.

The significance of each machining parameter change on the total response characteristic is determined by the percentage contribution of the corresponding machining parameter to the total sum of squared deviations SS_T. Alternatively, from the F value of the Fisher test (F-test), the larger F value indicates that the corresponding parameter has a significant impact on response characteristics.

Genetic Algorithm (GA)

For optimizing machining parameters, GA is widely used as it is a handy tool. For optimizing input parameters, this algorithm follows a population-based search method. After processing data by GA, the obtained output includes a set of chromosomes having an infinite length where every bit is called a gene. A fixed number of chromosomes are selected. They are called a population. For a fixed time, this population is called generation, and this generation of the primary population of chromosomes is chosen randomly. As the binary alphabet provides the maximum number of schemes per bit of information in any coding, it is usually used to denote the chromosomes using ones and zeros. Then each member is evaluated through the fitness function (objective function). By operating the population by reproduction, crossover, and mutation, a new population is created for further evaluation and then tested for optimization. The whole process can be divided into three steps for implementing optimization using GA. Coding, fitness function are the basic operators of GA. Obtained results after using GA are used to validate the multi-objective optimization results obtained from GRA optimization process [105].

For optimizing face milling parameters, the input parameters are encoded as genes by binary coding. Chromosomes are created with a set of genes used to perform basic GA mechanisms, namely, crossover, mutation. For creating new children, parts of chromosomes are exchanged. This process helps to explore the whole search space. The mutation is then done to provide randomness to the new chromosome to prevent losing essential information from the earlier stage. An objective function is needed for this face milling optimization process and for creating new generations. After performing several iterations, the optimal face milling parameters have been obtained. Weighting factors and constraints are also necessary for performing GA efficiently.

The objective function can be expressed as follows:

$$U(T,R,F_Y,M) = C_T\left(\frac{\mathrm{T'}-\mathrm{T_c}}{\mathrm{T_{max}}-\mathrm{T_c}}\right)+C_R\left(\frac{\mathrm{R_c}-\mathrm{R'}}{\mathrm{R_c}-\mathrm{R_{min}}}\right)+C_F\left(\frac{\mathrm{F_c}-\mathrm{F'}}{\mathrm{F_c}-\mathrm{F_{min}}}\right)+C_M\left(\frac{\mathrm{M'}-\mathrm{M_c}}{\mathrm{M_{max}}-\mathrm{M_c}}\right) \quad (3.11)$$

Here, M = MRR, F = Avg. F_Y, R= Ra, and T= tool life.

Subjected to, $\mathrm{T'} \geq \mathrm{T_c}$, $\mathrm{R_c} \geq \mathrm{R'}$, $\mathrm{F_c} \geq \mathrm{F'}$, $\mathrm{M'} \geq \mathrm{M_c}$

$$C_T + C_R + C_F + C_M = 1 \quad (3.12)$$

Here, C_T, C_R, C_F, C_M are weighting factors.

Experimentation

Workpiece and cutting tool material

Face milling experiments were conducted using the Ganesh VMC-1814 CNC milling machine. Ti6Al4V titanium alloy of hardness 315-345 BHN (Figure 4) has been used as the workpiece material and its composition is shown in Table 2. The workpieces were prepared in a dimension of 152.4 mm×101.6 mm ×101.6 mm (Figure 5 (a)). Square shaped carbide inserts were used in this study which were PVD coated with TiN+TiAlN (Figure 5 (b)). The inserts were of F40M grade with a 0° rake angle.

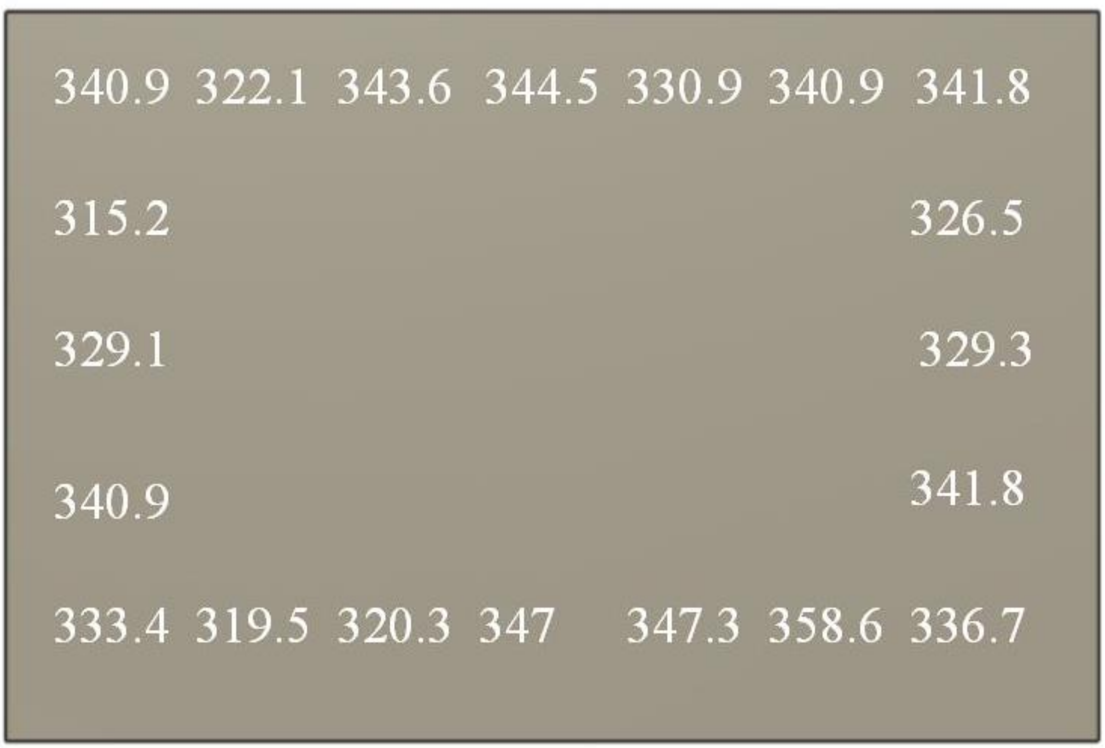

Figure 4. Brinell Hardness values on the workpiece surface

a b

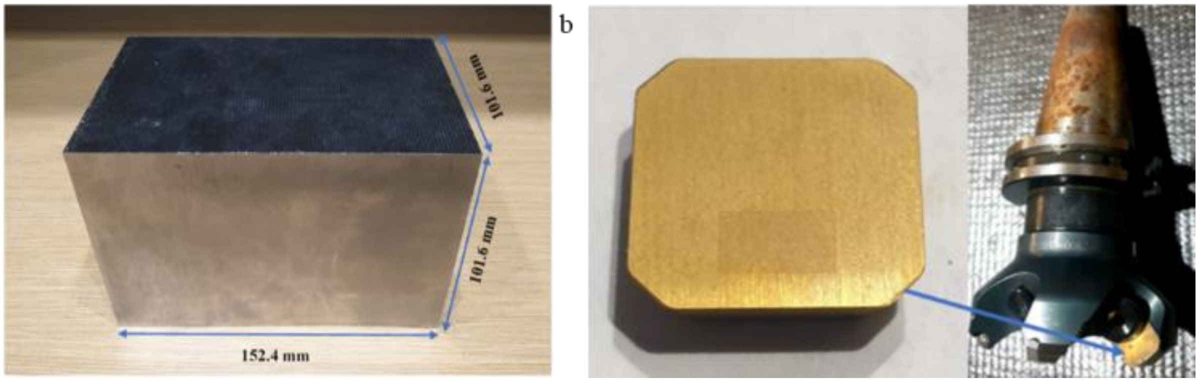

Figure 5. (a) workpiece; (b) cutting insert and tool holder.

Table 2. Composition of Ti6Al4V alloy.

Content	**Composition(%)**
Aluminum	6
Vanadium	4
Iron	.25
Oxygen	.2
Titanium	Balance

Design of Experiment using Taguchi Method

In this study, face milling experiments of titanium alloy is designed using the Taguchi design of experiment (DOE) where Taguchi's L9 orthogonal array is used. Cutting speed, feed rate, and radial depth of cut are selected as input factors while cutting forces, Ra, tool life, and MRR are considered as response characteristics. Levels of input factors and corresponding Taguchi's L9 orthogonal array are shown in Table 3, and Table 4, respectively. Levels of all the factors are determined based on some trial experiments and the axial depth of cut is kept constant at 2.54 mm.

Table 3: Factors and corresponding levels

Factors	Level 1	Level 2	Level 3
Cutting speed (m/min)	50	57.5	65
Feed rate (mm/rev)	0.2	0.25	0.3
Radial depth of cut (mm)	7.5	10	12.5

Table 4: DOE using Taguchi L_9 orthogonal array

Experiment	Level of factors		
	Cutting Speed	Feed rate	Radial Depth of cut
1	1	1	1
2	1	2	2
3	1	3	3
4	2	1	2
5	2	2	3
6	2	3	1
7	3	1	3
8	3	2	1
9	3	3	2

Cutting forces, surface roughness, and tool wear measurements

Kistler 9255C dynamometer has been used to measure the cutting forces. The dynamometer has been placed under a fixture specially made for holding the workpiece and a charge amplifier is used to transfer the corresponding force signals which are then processed using DynoWare software. A complete schematic diagram of the experimental setup and force measurements are shown in Figure 6 and Figure 7 respectively.

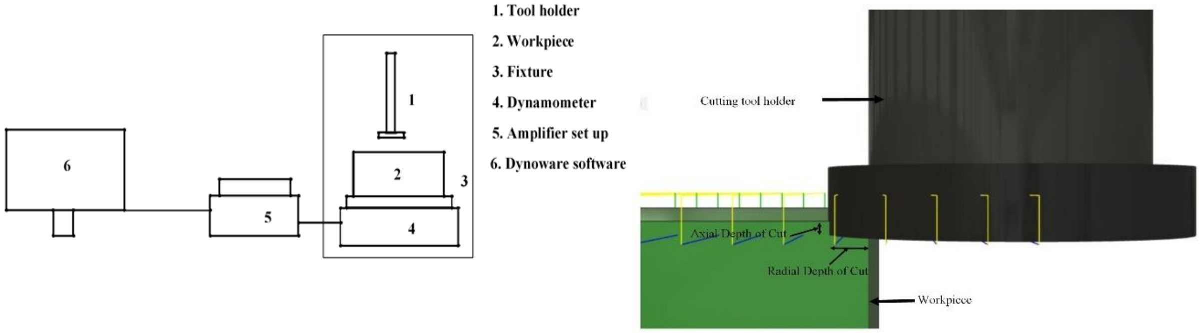

Figure 6. (a) Schematic diagram of the experimental setup, (b) Autodesk Fusion program for cutting Ti6Al4V

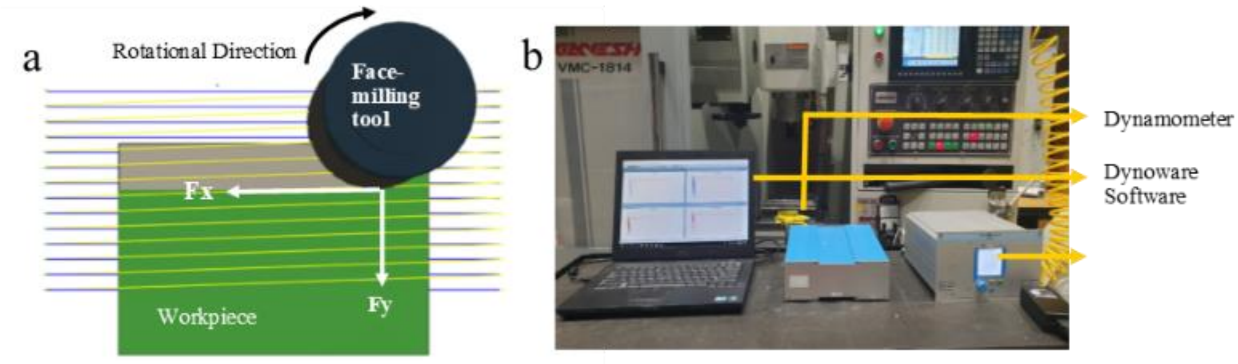

Figure 7. (a) Force measurement set up; (b) Tool path and cutting force direction.

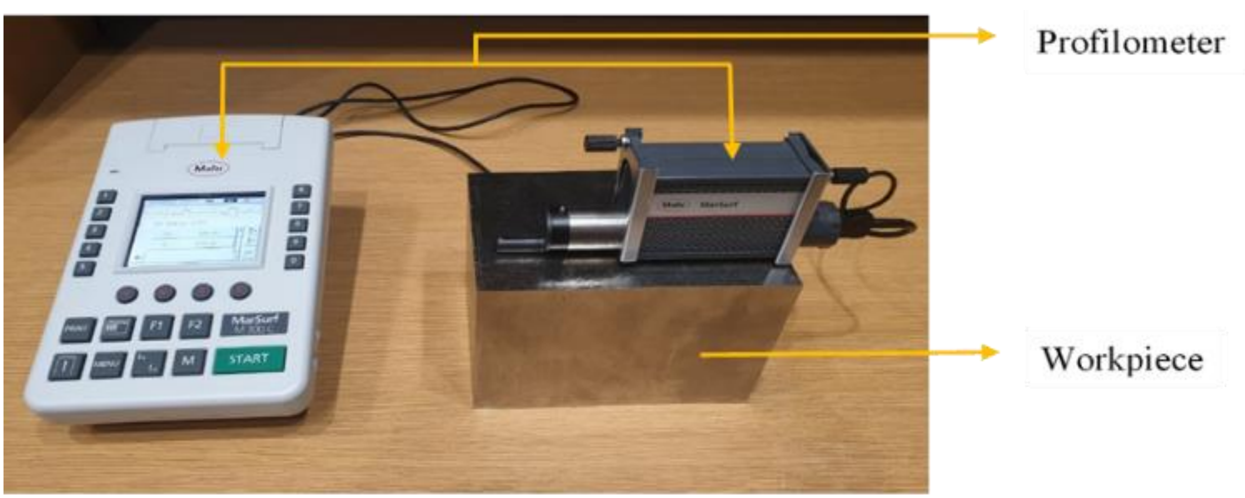

Figure 8. Surface roughness measurement set up.

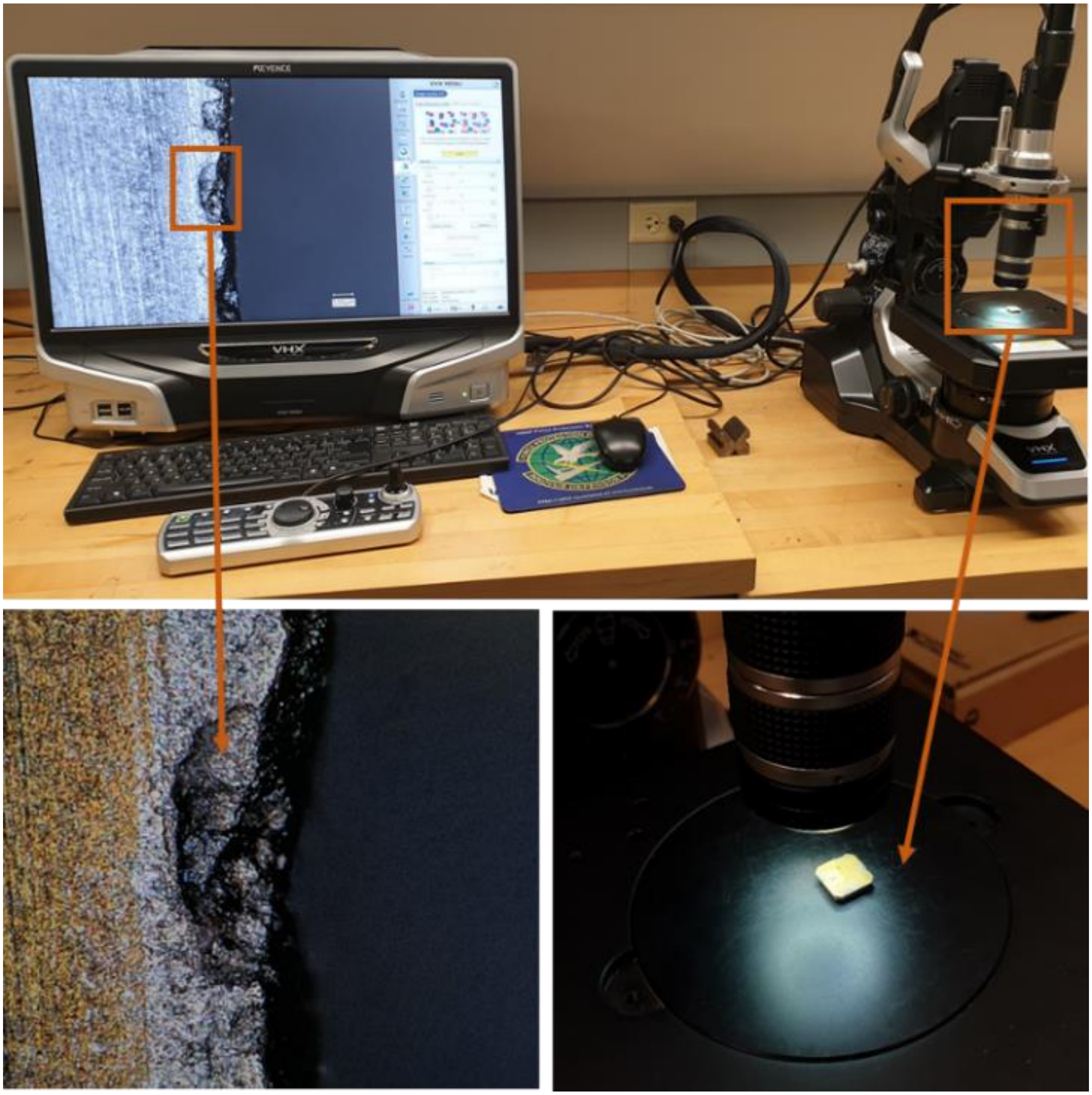

Figure 9. Tool wear measurement.

Tool wear has been measured using a Keyence VHX-5000 optical microscope. The maximum tool life corresponds to 0.3 mm flank wear. MahrSurf M 300 C profilometer has been used to measure the machined workpiece surface roughness value (Ra). Figure 8 and Figure 9 show Ra, and tool wear measurement setup, respectively.

CHAPTER IV

RESULTS AND DISCUSSION

Non-uniform flank wear has been found throughout the experiment. Figure 10 depicts the tool wear from the top view and 45° angle view to get a better observation. The wear in the minor cutting edge is too small to be considered as significant for measuring tool life, hence flank wear has been measured as the dominant tool wear to find the maximum tool life. When the flank wear reaches 300µm, the corresponding tool life is considered maximum. Flank wear has been measured each time after cutting 152.4 mm length of the workpiece.

a b
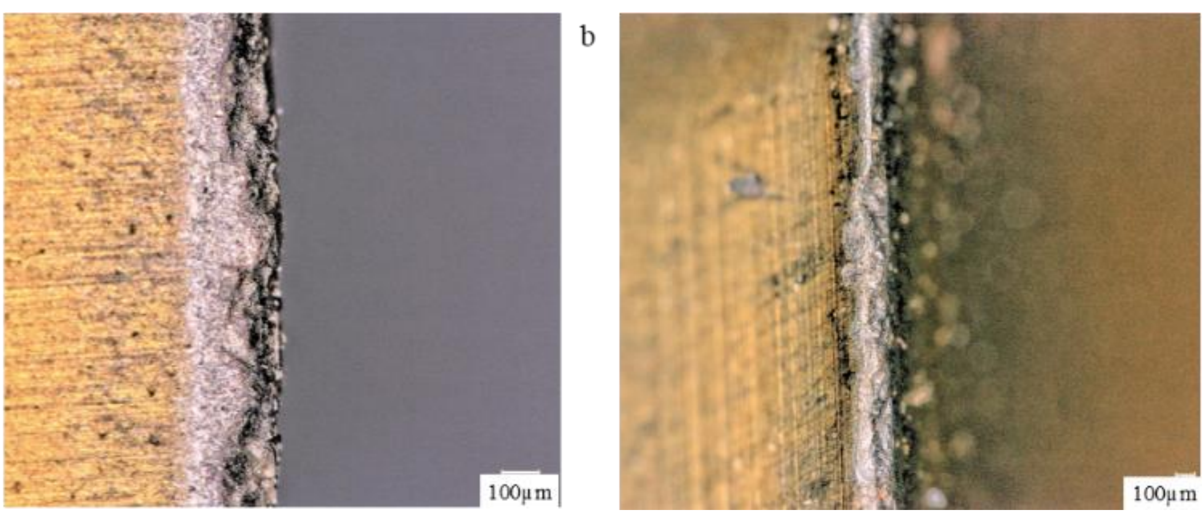

Figure 10. Tool wear during face milling of Ti6Al4V at feed rate 0.25 mm, cutting speed 50 m/min and radial depth of cut 10 mm (a) top view; (b) 45-degree angle view.

Figure 11 demonstrates the variation of flank wear with machining time at different machining parameters where a sharp increase in wear is found both at the beginning and the end of the experiments.

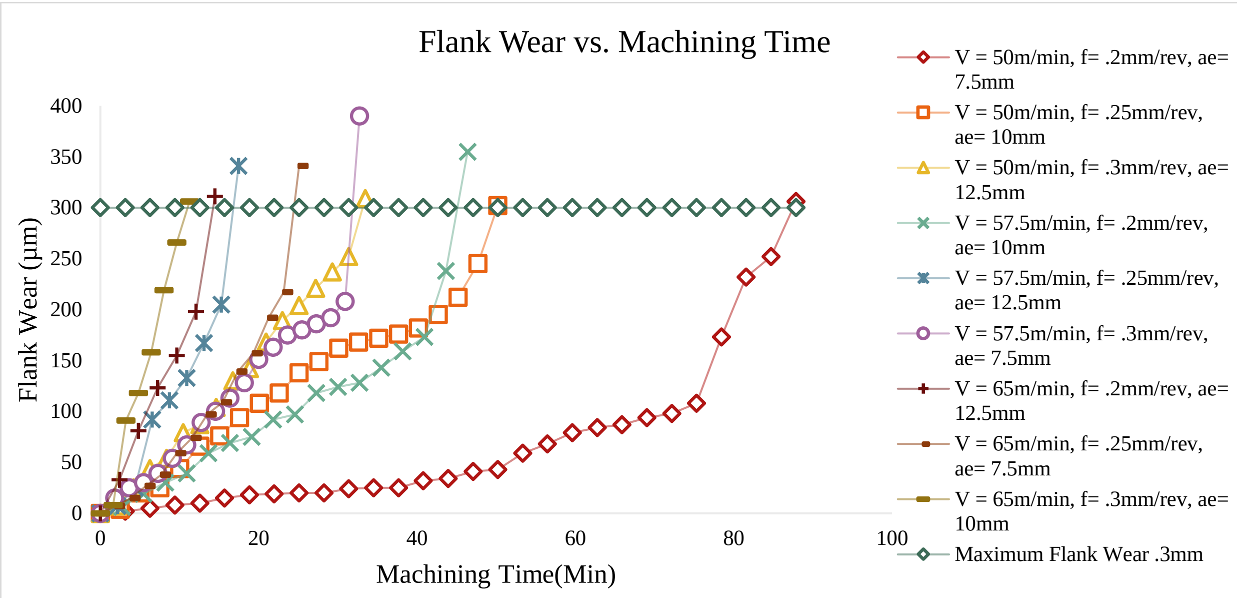

Figure 11. Variation of flank wear with machining time at different machining parameter values.

Ra is considered an important machining characteristic to evaluate machined surface quality. Although many factors can have significant impacts on the machined surface, parameters such as cutting speed, feed rate, and radial depth of cut are varied in this study to find an optimum average Ra. After cutting every 152.4 mm length of the workpiece, Ra has been measured at five different places of the machined surface and then an average value of Ra has been taken for every pass to draw the graph as shown in Figure 12. In the Ra vs. cutting time graph, some sharp changes have been observed in some places due to the fact that the hardness values of the workpiece material are not uniform throughout the whole workpiece [106]. An optical microscopic view of the machined surface is shown in Figure 13.

It is observed that the dynamic cutting forces have the most significant impact on tool wear during the face milling process. Increased Ra has been observed due to the vibrations created by the cutting forces.

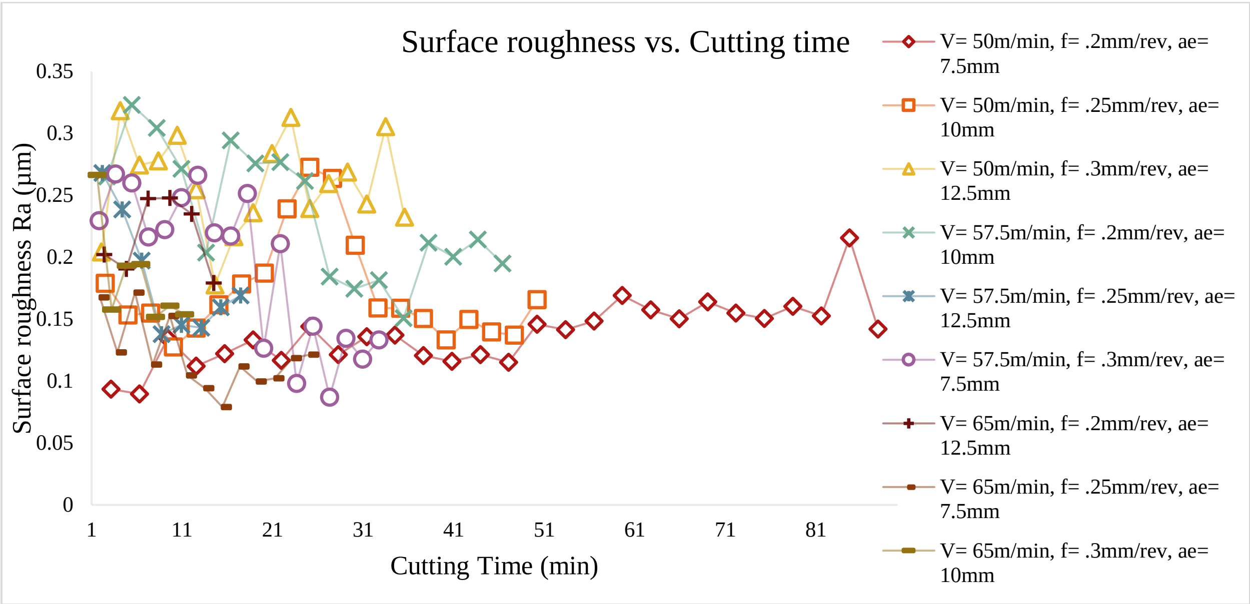

Figure 12. Average surface roughness vs. Machining time at different machining parameter values.

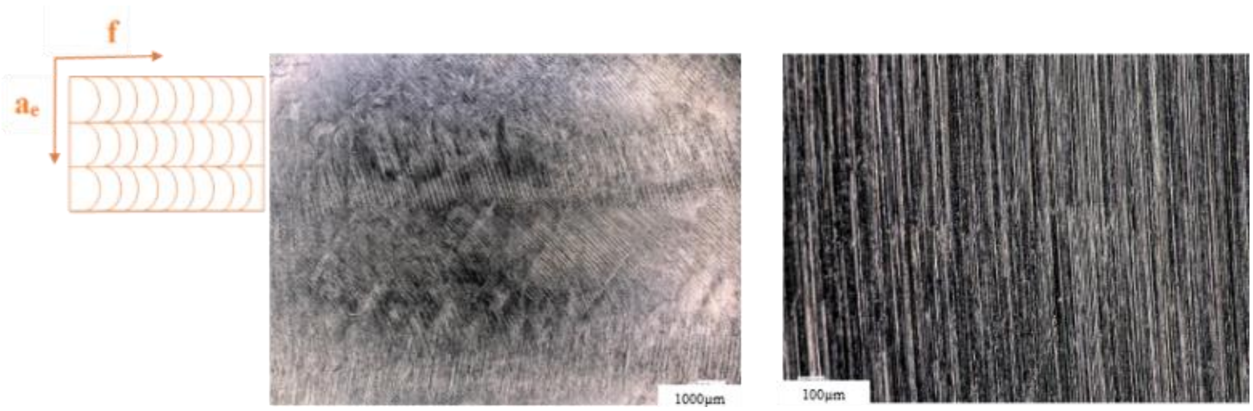

Figure 13. Optical Microscopic view of workpiece Surfaces at feed .2 mm/rev, cutting speed 50 m/min, and radial depth of cut 7.5 mm.

Average cutting forces (Avg. Fx, Avg. Fy, and Avg. Fz) are measured in X, Y, and Z directions as shown in Figure 14. Avg. F_Z is not considered during process optimization. Avg. F_X and Avg. F_Y are measured for each 152.4 mm pass and used for the analysis which are shown in Figure 15 and Figure 16 respectively.

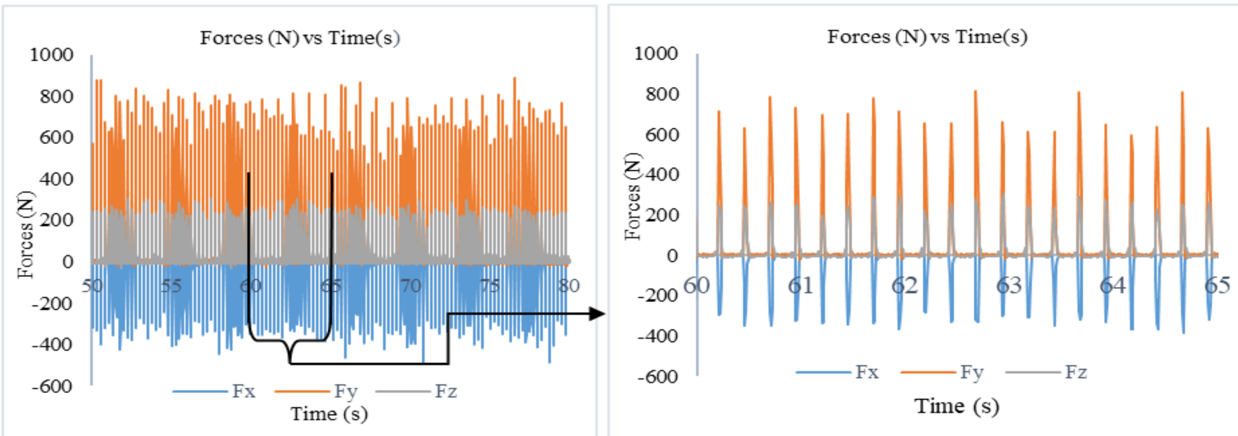

Figure 14. Cutting forces vs. Time graph obtained at feed rate 0.2 mm/rev, cutting speed 50 m/min, and radial depth of cut 7.5 mm.

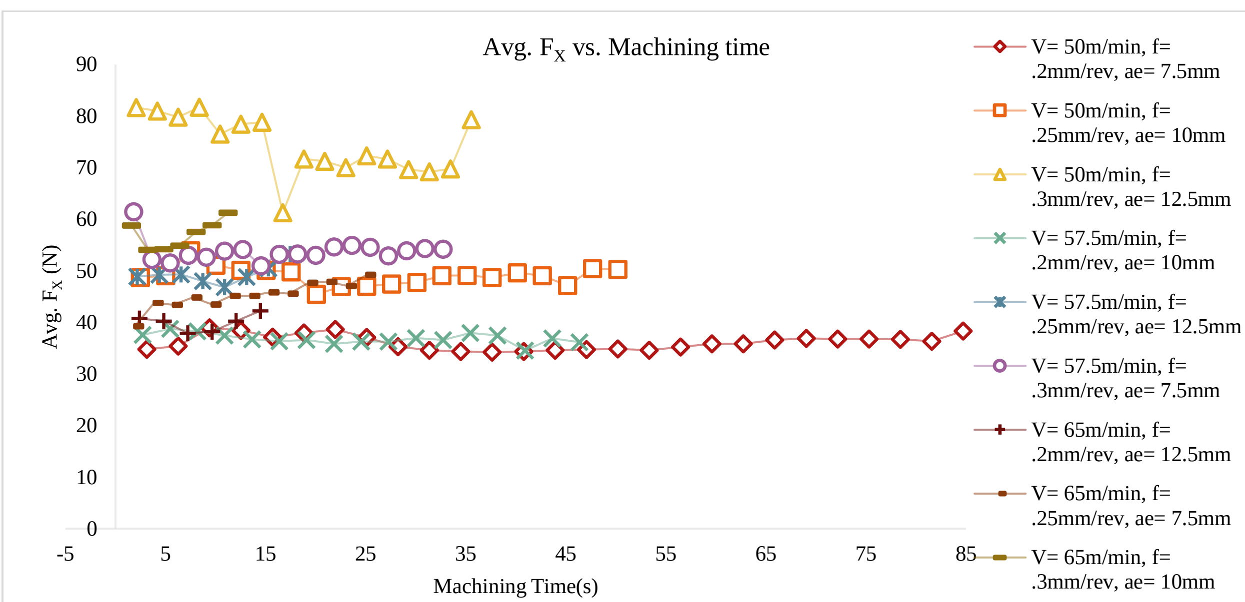

Figure 15. Avg. F_X vs. Machining time at different machining parameter values.

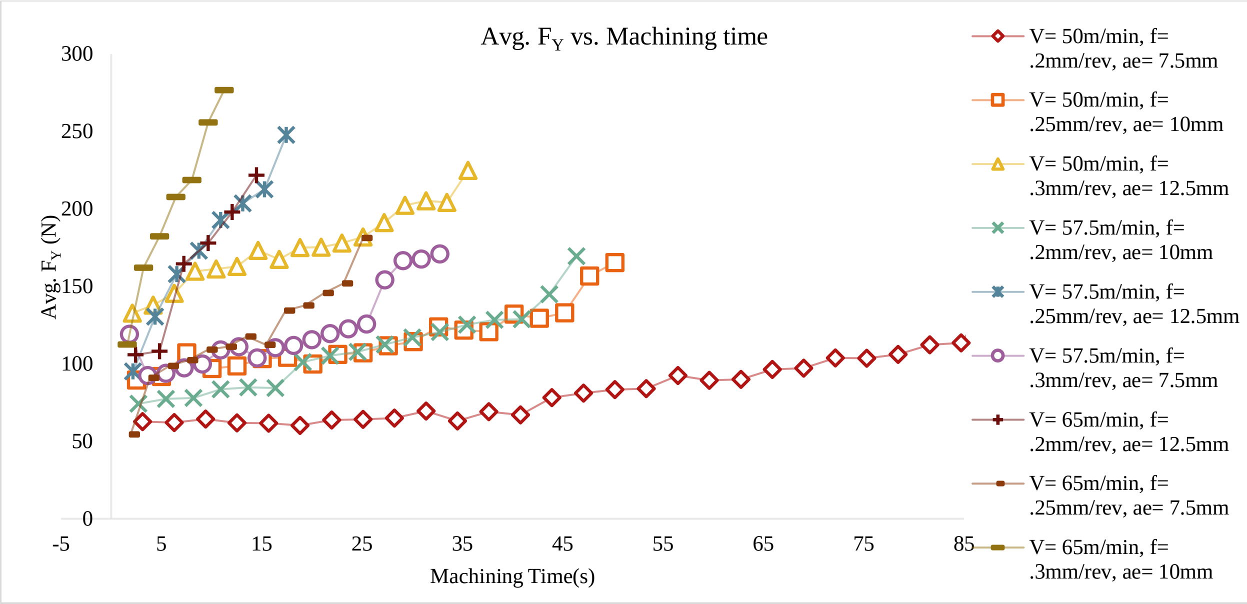

Figure 16. Avg. F_Y vs. Machining time at different machining parameter values.

Signal to Noise (S/N) ratio analysis

Minitab 19 software has been used to perform the Taguchi and regression analysis. The impact of each level of input parameter on the output characteristics is analyzed using the S/N ratio based on equation (3. 1) and (3. 2). During the optimization of cutting forces and Ra the smaller the better characteristic is chosen and for tool life and MRR the larger the better characteristic is chosen which are shown in Table 5. Figure 23 illustrates the main effects of S/N ratios, where the optimal parameters are highlighted in red circles. The highest S/N ratio indicates the optimal level.

Table 5: Experiment and S/N (dB) results

Experiment Number	Tool Life (min)	Ra (μm)	Avg. F_X (N)	Avg. F_Y (N)	MRR (cm^3/min)
1	87.860	0.138	36.080	82.450	9.234
2	50.200	0.173	49.040	115.710	15.389
3	33.470	0.260	74.350	175.250	23.084
4	56.390	0.147	36.140	108.460	14.158
5	17.460	0.182	49.360	176.690	22.122
6	32.740	0.192	53.822	121.800	15.928
7	14.480	0.153	39.938	162.740	20.006
8	25.100	0.119	45.258	119.070	15.005
9	11.260	0.182	57.091	202.300	24.007

Figure 17 (a) demonstrates that the optimum parameter setting for tool life is A1B1C1 during the face milling of Ti6Al4V. So, using 50 m/min cutting speed, 0.2 mm/rev feed rate, and 7.5 mm radial depth of cut the maximum tool life can be obtained. Tool life has decreased with the increase of cutting speed, feed rate, and depth of cut. Higher cutting speed generates higher temperatures at the cutting zone which reduces the tool strength resulting in plastic deformation. Therefore, higher cutting speed results in higher tool wear. A similar result is found in the study of the face milling of titanium alloy with coated carbide tools [107]. With the increase of feed rate and radial depth of cut, the cutting forces increase [3] which leads to faster tool wear and reduced tool life. From the literature review, a similar result is found [108]. Compared to the cutting speed the effect of radial depth of cut on tool life is smaller.

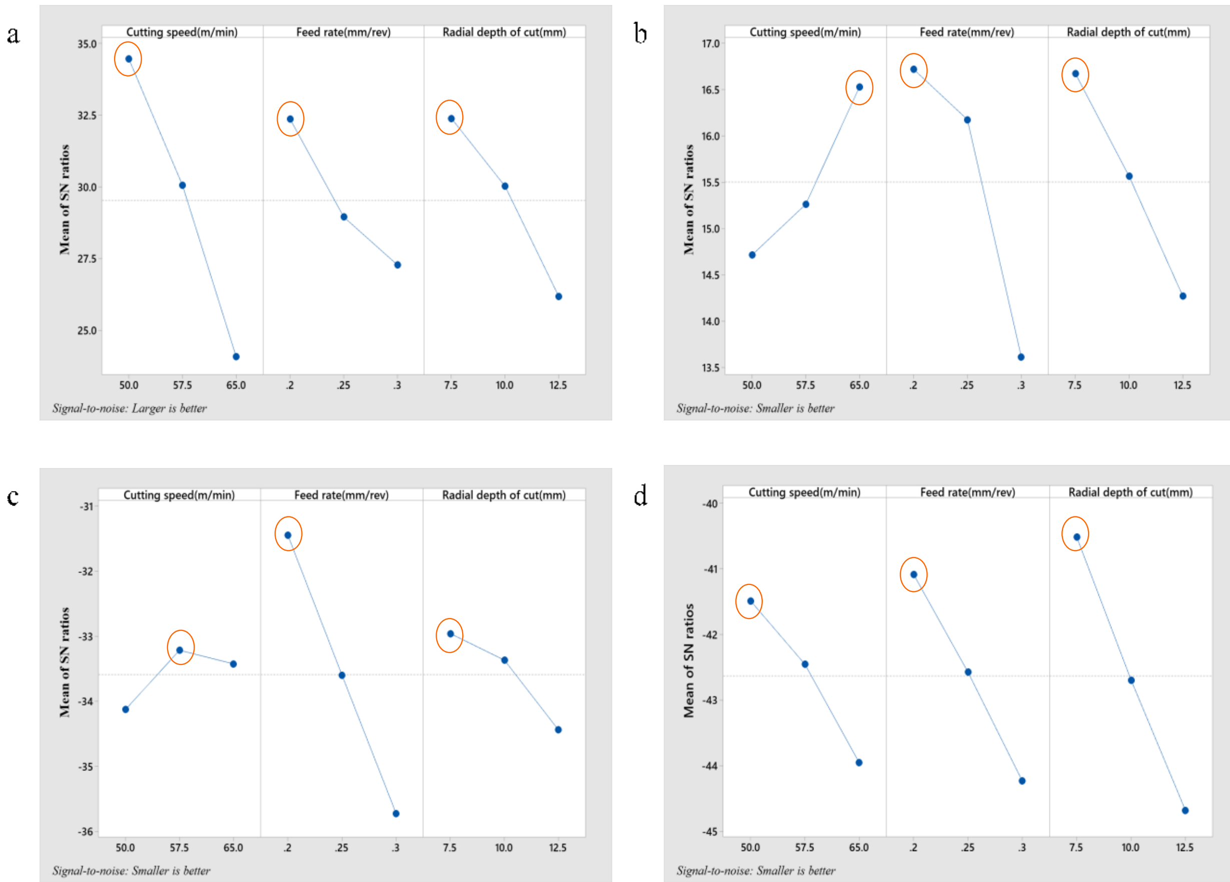

Figure 17. Main effects plot of S/N ratios for (a) Tool life, (b) Ra, (c) Avg. F_X, (d) Avg. F_Y during face milling of Ti6Al4V.

The optimal condition of cutting parameters for Ra is A3B1C1 as shown in Figure 17 (b), which corresponds to cutting speed 65 m/min, feed rate 0.2 mm/rev, and radial depth of cut 7.5 mm. Ra increases with the decrease of cutting speed and with the increase of feed rate and radial depth of cut. Higher cutting speed results in higher temperatures in the cutting zone which softens the workpiece material. As a result, machining vibration reduces, and therefore Ra reduces. A higher feed rate increases mechanical load and MRR resulting in higher vibrations and material resistance respectively, therefore, the surface quality deteriorates. A similar study is found in the literature [109]. With the decrease of radial depth of cut, the contact area between tool and workpiece decreases resulting in a reduction in friction between the cutting tool and workpiece surface. As a result, the average Ra value decreases.

The optimal condition for Avg. F_X is A2B1C1 as shown in Figure 17 (c), which corresponds to cutting speed 57.5 m/min, feed rate 0.2 mm/rev, and radial depth of cut 7.5 mm and optimum setting for Avg. F_Y is A1B1C1 as shown in Figure 17 (d), which corresponds to cutting speed 50 m/min, feed rate 0.2 mm/rev, and radial depth of cut 7.5 mm. With the increase of feed rate and depth of cut both Avg. F_X and Avg. F_Y increase. For Avg. F_X, the force has decreased initially and then starts to increase again with the increase of cutting speed. For Avg. F_Y, the force increases with the increase in cutting speed. Higher feed rate and radial depth of cut result in a larger contact area and contact length between the workpiece and cutting tool which raises the cutting forces. A similar study has been obtained from the literature search [110].

Analysis of Variance

For evaluating the significant factors which affect the expected response parameters, Analysis of Variance (ANOVA) is performed using a 95% confidence level. Results of ANOVA analysis are shown in Table 6, Table 7, Table 8, and Table 9.

Based on Table 6, cutting speed has the highest impact on tool life. Cutting speed has shown a significant contribution of 50.06%, and feed rate and radial depth of cut have shown 25.59% and 22.80%, respectively. From the experimental findings shown in Figure 17 (a) the highest S/N ratio (34.461) has been found for the lowest cutting speed which is consistent with ANOVA analysis. F values have shown that all the input parameters are statistically significant for tool life.

Table 6: ANOVA results for Tool life (min)

Source	DF	Seq SS	Adj SS	Adj MS	F Value, $\alpha < 0.05$	Contribution
Cutting speed (m/min)	2	2432.37	2432.37	1216.19	32.32	50.06%
Feed rate (mm/rev)	2	1243.22	1243.22	621.61	16.52	25.59%
Radial depth of cut (mm)	2	1108.01	1108.01	554.00	14.72	22.80%
Error	2	75.26	75.26	37.63		1.55%
Total	8	4858.87				100.00%

SS = Sum of Squares; Adj SS= Adjusted Sum of Squares; Adj MS = Adjusted Mean of Squares; DF = Degree of Freedom

According to Table 7, the impact of cutting speed, feed rate, and radial depth of cut on Ra are 17.28%, 54.58%, and 27.39%, respectively. So, the feed rate is the most influential parameter for Ra. The same result is obtained from the experimental analysis shown in Figure 17 (b) where the highest S/N ratio has been obtained for the lowest feed rate (16.72 dB). From the literature, a similar result is found [93]. All the input parameters are found statistically significant for Ra according to their F values.

Table 7: ANOVA results for Ra (µm).

Source	DF	Seq SS	Adj SS	Adj MS	F-Value, $\alpha < 0.05$	Contribution
Cutting speed (m/min)	2	0.002298	0.002298	0.001149	23.08	17.28%
Feed rate (mm/rev)	2	0.007257	0.007257	0.003628	72.89	54.58%
Radial depth of cut (mm)	2	0.003642	0.003642	0.001821	36.58	27.39%
Error	2	0.000100	0.000100	0.000050		0.75%
Total	8	0.013296				100.00%

From Table 8, it is found that Avg. F_X is mostly influenced by feed rate. Cutting speed, feed rate, and radial depth of cut have 6.80%, 77.28%, and 12.64% contributions, respectively. From the F values, it is found that the feed rate is the most significant parameter that affects Avg. F_X. Similarly, the experimental analysis also (Figure 17 (c)) shows that the lowest feed rate has provided the maximum S/N ratio (-31.44 dB). A similar result is found in the previous study [94]. However, the radial depth of cut is found insignificant for Avg. F_X.

Table 8: ANOVA results for Avg. F_X (N)

Source	DF	Seq SS	Adj SS	Adj MS	F-Value, $\alpha < 0.05$	Contribution
Cutting speed (m/min)	2	78.88	78.88	39.44	2.07	6.80%
Feed rate (mm/rev)	2	896.40	896.40	448.20	23.56	77.28%
Radial depth of cut(mm)	2	146.57	146.57	73.28	3.85	12.64%
Error	2	38.04	38.04	19.02		3.28%
Total	8	1159.89				100.00%

The most important machining parameter for Avg. F_Y is the radial depth of cut and it has a 48.34% contribution as shown in Table 9. The contributions of cutting speed and feed rate were 16.98%, and 28.36%, respectively. From the F values, it can be concluded that only radial depth of cut and feed rate are statistically significant. A previous study also showed similar results [92].

Table 9: ANOVA results for Avg. F_Y (N)

Source	DF	Seq SS	Adj SS	Adj MS	F-Value, $\alpha < 0.05$	Contribution
Cutting speed (m/min)	2	2148.1	2148.1	1074.0	2.69	16.98%
Feed rate (mm/rev)	2	3588.2	3588.2	1794.1	4.49	28.36%
Radial depth of cut (mm)	2	6115.5	6115.5	3057.7	7.65	48.34%
Error	2	799.1	799.1	399.5		6.32%
Total	8	12650.9				100.00%

Regression Analysis

Statistical software Minitab 19 is used for developing mathematical models and the first-order models which are illustrated here and their results are shown compared with the actual results from the experiments in Figure 18, Figure 19, Figure 20, Figure 21, and Figure 22.

$$\text{Tool life (min)} = 312.0 - 2.682\ \mathrm{V}_c - 270.9\ \mathrm{f} - 5.35\ \mathrm{a}_e \tag{4. 1}$$

$R^2 = 94.73\%; R^2(\text{adj}) = 91.56\%$

$$R_a(\mu\text{m}) = 0.0606 - 0.002600\ \mathrm{V}_c + 0.653\ \mathrm{f} + 0.00973\ \mathrm{a}_e \tag{4. 2}$$

$R^2 = 92.04\%; R^2(\text{adj}) = 87.26\%$

$$Avg.F_X\ (N) = -8.9 - 0.382\ \mathrm{V}_c + 243.7\ \mathrm{f} + 1.899\ \mathrm{a}_e \tag{4. 3}$$

$R^2 = 92.70\%; R^2(\text{adj}) = 88.32\%$

$$Avg.F_Y\ (N) = -249.9 + 2.460\ \mathrm{V}_c + 486\ \mathrm{f} + 12.76\ \mathrm{a}_e \tag{4. 4}$$

$R^2 = 92.35\%; R^2(\text{adj}) = 87.76\%$

$$MRR\ \left(\frac{cm^3}{min}\right) = -29.84 + 2.514\ \mathrm{V}_c + 6.54\ \mathrm{f} + 1.67\ \mathrm{a}_e \tag{4. 5}$$

$R^2 = 98.16\%; R^2(\text{adj}) = 97.06\%$

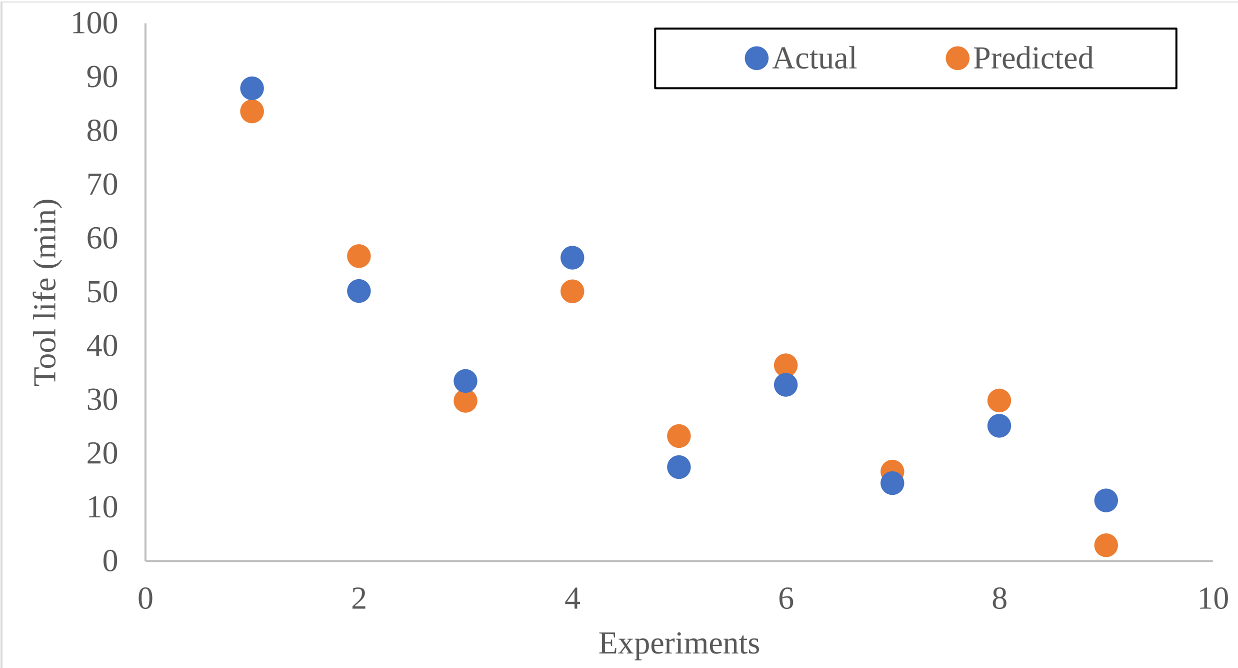

Figure 18. Actual and predicted values obtained from experiments and equation (4. 1)

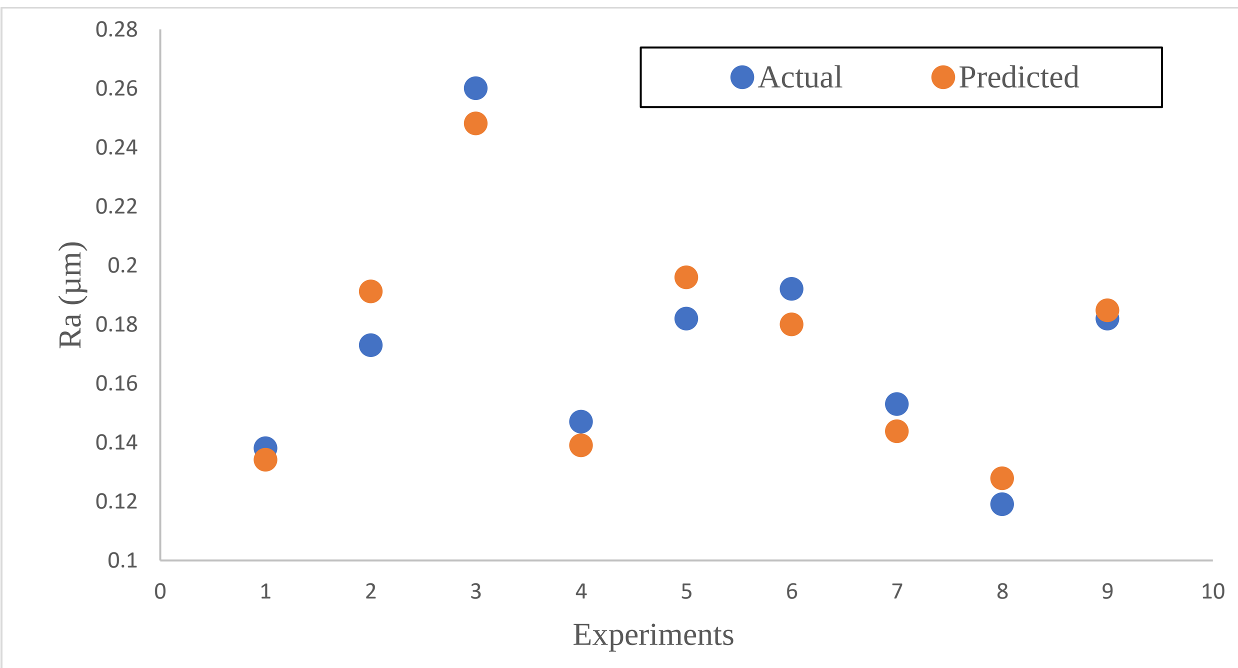

Figure 19. Actual and predicted values obtained from experiments and equation (4. 2)

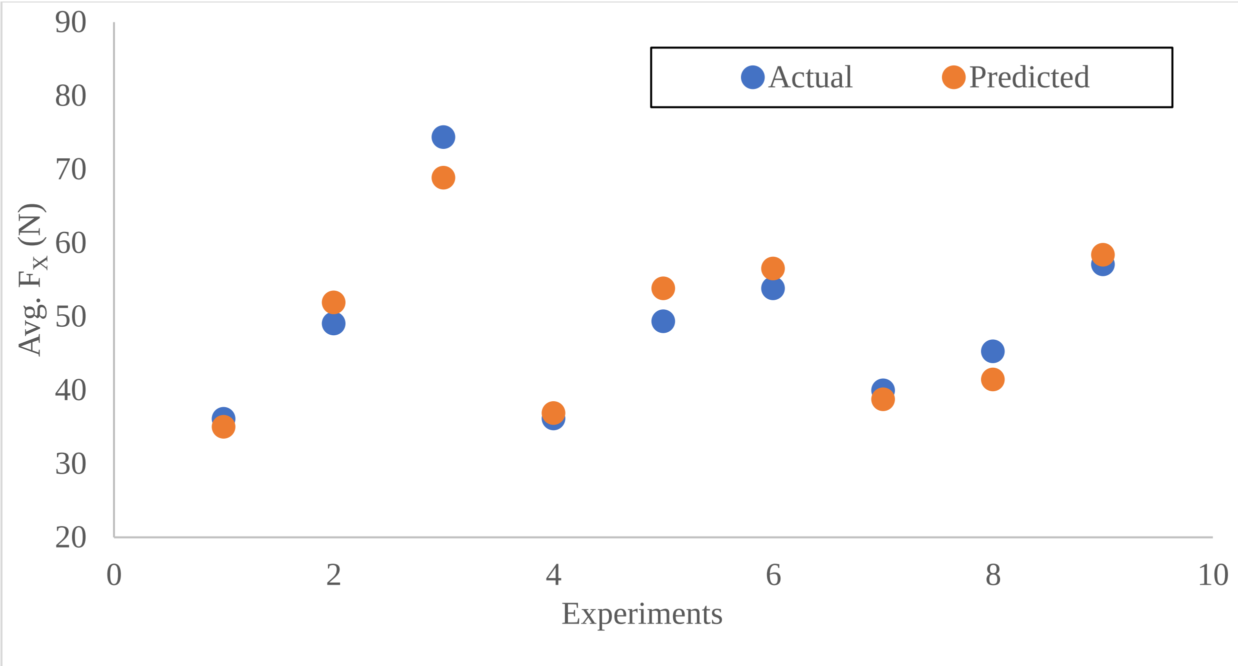

Figure 20. Actual and predicted values obtained from experiments and equation (4. 3)

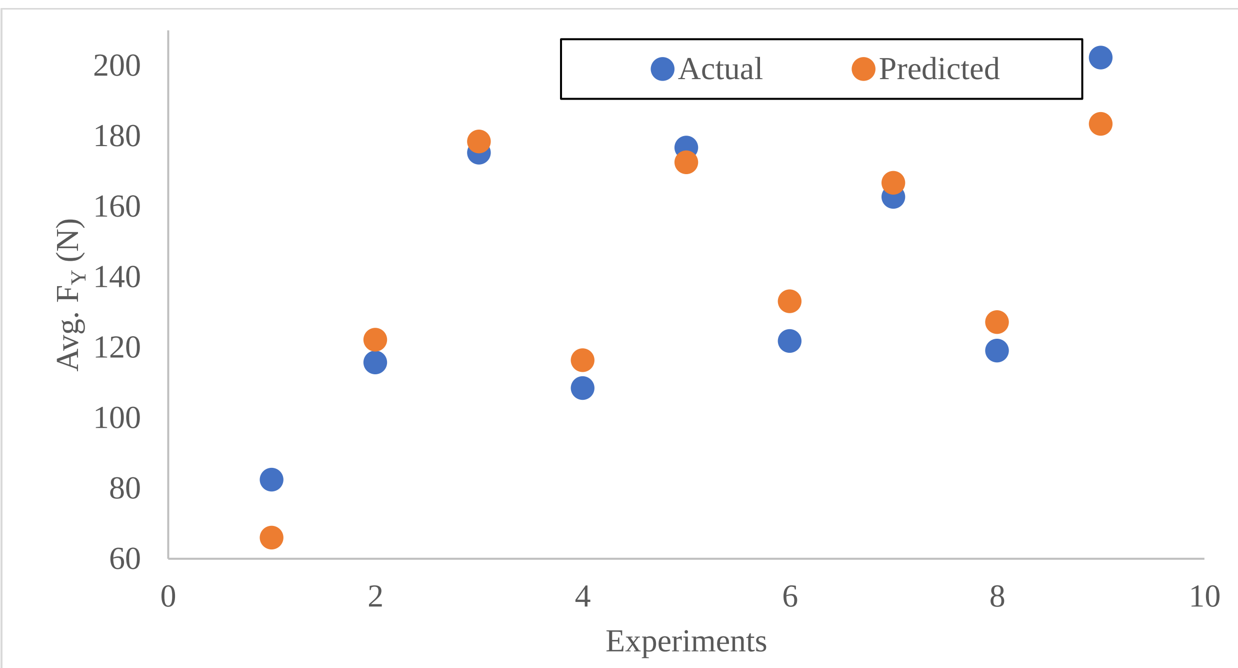

Figure 21. Actual and predicted values obtained from experiments and equation (4. 4)

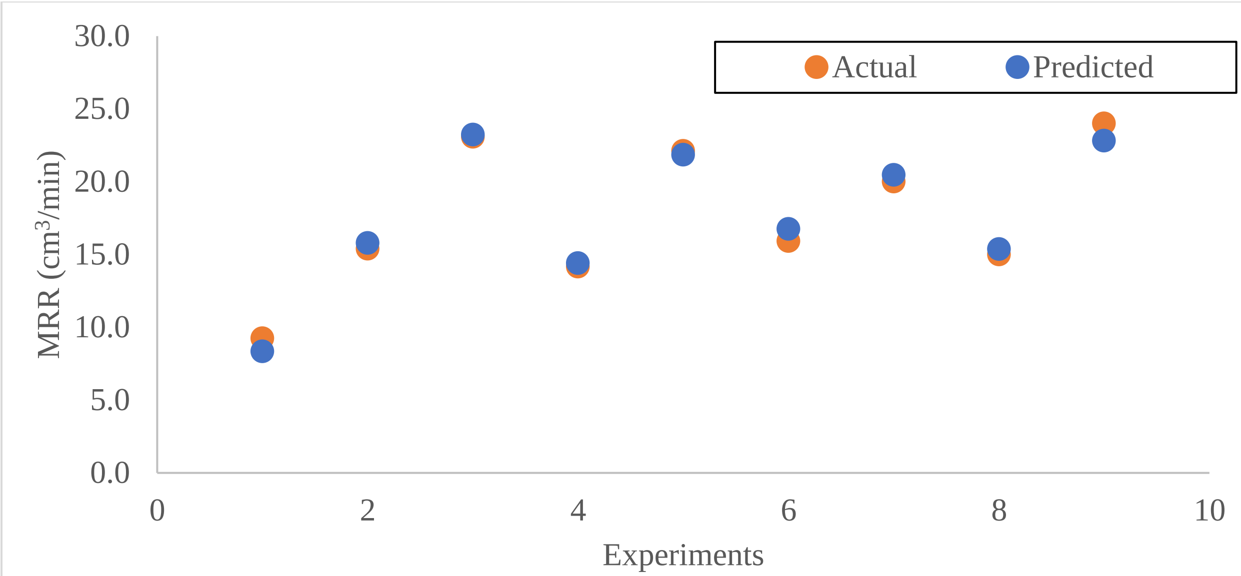

Figure 22. Actual and predicted values obtained from experiments and equation (4. 5)

Grey Relational Analysis

Combining the data of different levels of factors, a level average analysis has been performed to explain the results. The greatest difference between the highest and lowest average response of any factor is defined as the measurement of the largest effect of that factor. Data preprocessing has been performed for all the response characteristics using equations (3. 3) and (3. 4) and the corresponding results are shown in Table 10. Grey Relational coefficient and Grey Relational Grade are computed using equations (3. 5) and (3. 6) respectively which are shown in Table 11. Tool life, Ra, and Avg. F_Y are considered for multi-objective (three objectives) optimization in this study.

Table 10: Data preprocessing for each performance characteristics

Run	Tool life $\delta_{Oi}(1)$	Avg. F_Y $\delta_{Oi}(2)$	Ra $\delta_{Oi}(3)$
1	1.000	1.000	0.865
2	0.508	0.722	0.617
3	0.290	0.226	0.000
4	0.589	0.783	0.801
5	0.081	0.214	0.553
6	0.280	0.672	0.482
7	0.042	0.330	0.759
8	0.181	0.694	1.000
9	0.000	0.000	0.553

The difference between the high and low effect of each factor is used to find the statistic delta and then a classification has been done for finding the foremost influential factor. This process converts the multi-objective optimization problem into a one-objective optimization problem. The condition having a higher grey relational grade will be nearer to the optimal condition. Using the grey relational grade values obtained in Table 11, the mean of each level of the factors and the total mean of the grey relational grade are calculated, which are shown in Table 12. By using the main effect analytical computation method, a response graph is obtained (Figure 23) which shows that the optimal condition for these experiments is A1B1C1 which corresponds to 50 m/min cutting speed, 0.2 mm feed per revolution, and 7.5 mm radial depth of cut. According to Table 12, the radial depth of cut has the largest effect on the response characteristics while feed rate and cutting speed are the second and third, respectively.

Table 11: Grey relational coefficient (ξ_i) of each performance output and Grey relational grade (ψ_i)

Run	Grey Relational Coefficient			Grey Relational Grade	Rank
	Φ (1)	Φ (2)	Φ (3)	ψ_i	
1	1.000	1.000	0.788	0.929	1
2	0.504	0.643	0.566	0.571	3
3	0.413	0.392	0.333	0.380	9
4	0.549	0.697	0.716	0.654	4
5	0.352	0.389	0.528	0.423	7
6	0.410	0.604	0.392	0.502	5
7	0.343	0.427	0.580	0.482	6
8	0.379	0.621	1.000	0.667	2
9	0.333	0.333	0.427	0.398	8

Here, distinguishing coefficient ζ= 0.5 is considered.

Table 12: Response table Grey relational grade values

Level	Cutting Speed	Feed	Radial depth of cut
1	0.627	0.688	0.699
2	0.526	0.554	0.541
3	0.515	0.427	0.428
Delta	0.112	0.261	0.271
Rank	3	2	1

Total mean grey relational grade 0.556

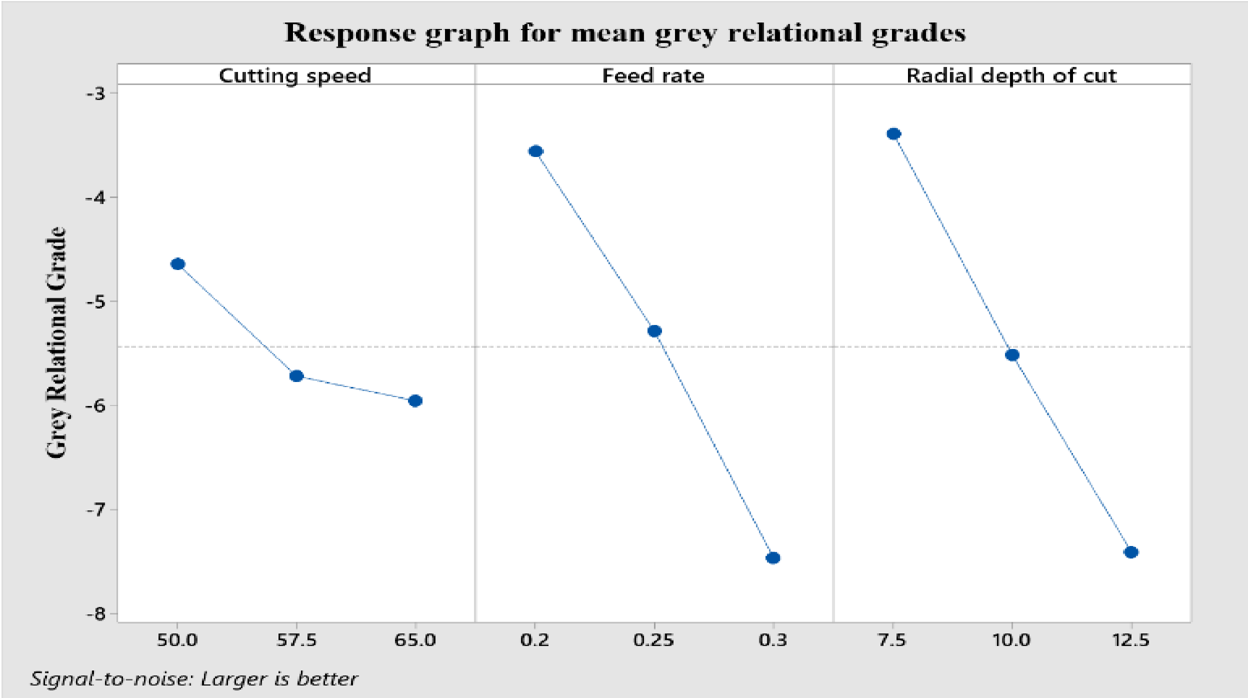

Figure 23. Response graph for mean grey relational grades.

Table 13: ANOVA results for process factors

Source	DF	Seq SS	Adj SS	Adj MS	F-Value	Contribution
Cutting speed (m/min)	2	0.023	0.023	0.011	3.28	9.25%
Feed rate (mm/rev)	2	0.103	0.103	0.051	14.98	42.23%
Radial depth of cut (mm)	2	0.111	0.111	0.056	16.21	45.71%
Error	2	0.007	0.007	0.003		2.82%
Total	8	0.243				100.00%

From the ANOVA analysis shown in Table 13, it is observed that feed rate and radial depth of cut have 42.23% and 45.71% contribution respectively. The F value obtained from Table 12 infers that feed rate and radial depth of cut are the most significant factors affecting the multiple performance characteristics. The results also indicate that cutting speed has no significant impact on performance characteristics.

Confirmation Experiment

Prediction and Validation for the Taguchi Analysis

The last stage of Taguchi analysis is to conduct an additional experiment to validate the predicted response values which are called a confirmation experiment. The confirmation experiment is conducted at the optimal parameters obtained during the analysis of Ra. The predicted values for Tool life, Ra, Avg. F_X, and Avg. F_Y are obtained from equations (4. 1), (4. 2), (4. 3), and (4. 4) respectively which are compared with the measured values from the confirmation experiment as shown in Figure 24 (a-d). In A3B1C1 validation experiment, the average percentage error for tool life, Ra, Avg. F_X and Avg. F_Y are 0.39%, 6.32%, 0.13% and 10.59%, respectively. The percent improvement of Ra at optimal condition is 31.29% shown in Table 14.

Table 14: Results of confirmation experiments

Response Parameter	Initial Setting (A2B1C3)	Optimal Setting (A3B1C1)	Percentage Improved
Ra (μm)	0.147	0.101	31.29%

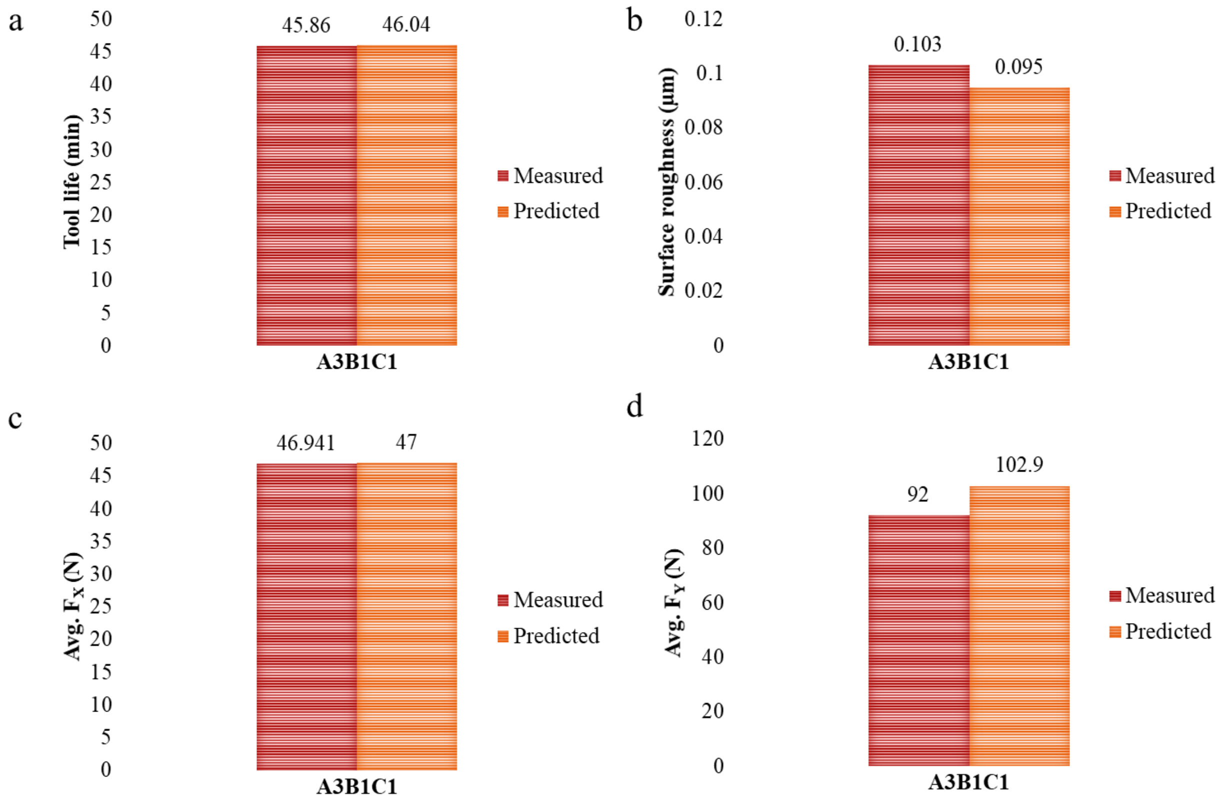

Figure 24. Results of confirmation experiments (a) Tool life, (b) Ra, (c) Avg. F_X, (d) Avg. F_Y.

It is observed that the predicted values obtained from the developed mathematical models in this study are very close to the measured results from the confirmation experiment. Thus, it can be concluded that the mathematical models found in this study can be used for predicting tool life, Ra, and cutting forces in the face milling of Ti6Al4V alloy.

Prediction and Validation for the Grey Relational Analysis

After selecting the optimal level of each factor, the final stage is to predict the output characteristics based on the optimal level of factors. Grey Relational Grade is predicted using the following equation-

$$\hat{\theta} = \theta_m + \sum_{i}^{k} \left(\overline{\theta_i} - \theta_m \right) \tag{4. 6}$$

θ is the estimated grey relational grade, θ_m the mean of the grey relational grade, θ_i is the mean of the grey relational grade at the optimal level, k is the number of machining parameters that significantly impact the multiple response characteristics. The grey relational grade can be predicted using equation (4. 6) for optimal cutting parameters even when the combination of input parameters cannot be found in the orthogonal array.

Comparison results of output responses at initial and optimal settings are shown in Table 15, where it is found that the tool life, Ra, and Avg. F_Y have improved by 55.81%, 6.12%, and 23.9% respectively.

Table 15: Results of output responses at an initial and optimal setting using GRA

	Initial Condition	Optimal Output characteristics		
		Prediction	Experiment	Percent Improved
Level	A2B1C3	A1B1C1	A1B1C1	
Tool Life (min)	56.39		87.86	55.81%
Ra (μm)	0.147		0.138	6.12%
Avg. F_Y (N)	108.46		82.45	23.98%
Grey Relational Grade	0.654	0.831	0.929	
Improvement of Grey Relational Grade	0.275			

Genetic Algorithm and Grey relational analysis results comparison

For both analyses, four response characteristics are chosen here: tool life, Ra, Avg. F_Y, and MRR. The following optimization is based on considering four objectives. Table 16 represents the range of input parameters used for the optimization process with GA tool.

Table 16: Range of Input parameters

Factors	Upper Bound	Lower Bound
Cutting Speed (m/min)	65	50
Feed rate (mm/rev)	.3	.2
Radial depth of cut (mm)	12.5	7.5

For roughing, equation (3.11) is used as the objective function and equation (4. 1), (4. 2), (4. 4),(4. 5) are used as constraints. Weighting factor, C_T = .3, C_R = .1, C_F = .1, C_M = .5 are considered. These constraints are used $T' \geq 11.26, .26 \geq R', 202.3 \geq F', M' \geq 9.234$.

For finishing, equation (3.11) is used as the objective function and equation (4. 1), (4. 2), (4. 4), (4. 5) are used as constraints. Weighting factor, C_T = .2, C_R = .6, C_F = .1, C_M = .1 are considered. These constraints are used $T' \geq 11.26, .15 \geq R', 150 \geq F', M' \geq 9.234$.

Population size 20, Elit count 2, generation 100, crossover fraction 0.8, and mutation rate 0.01 are used for both optimization and for roughing and finishing, 55 and 61 iterations are illustrated in Figure 25 (a) and (b), respectively. The final optimized results using GA tool are shown in Table 23.

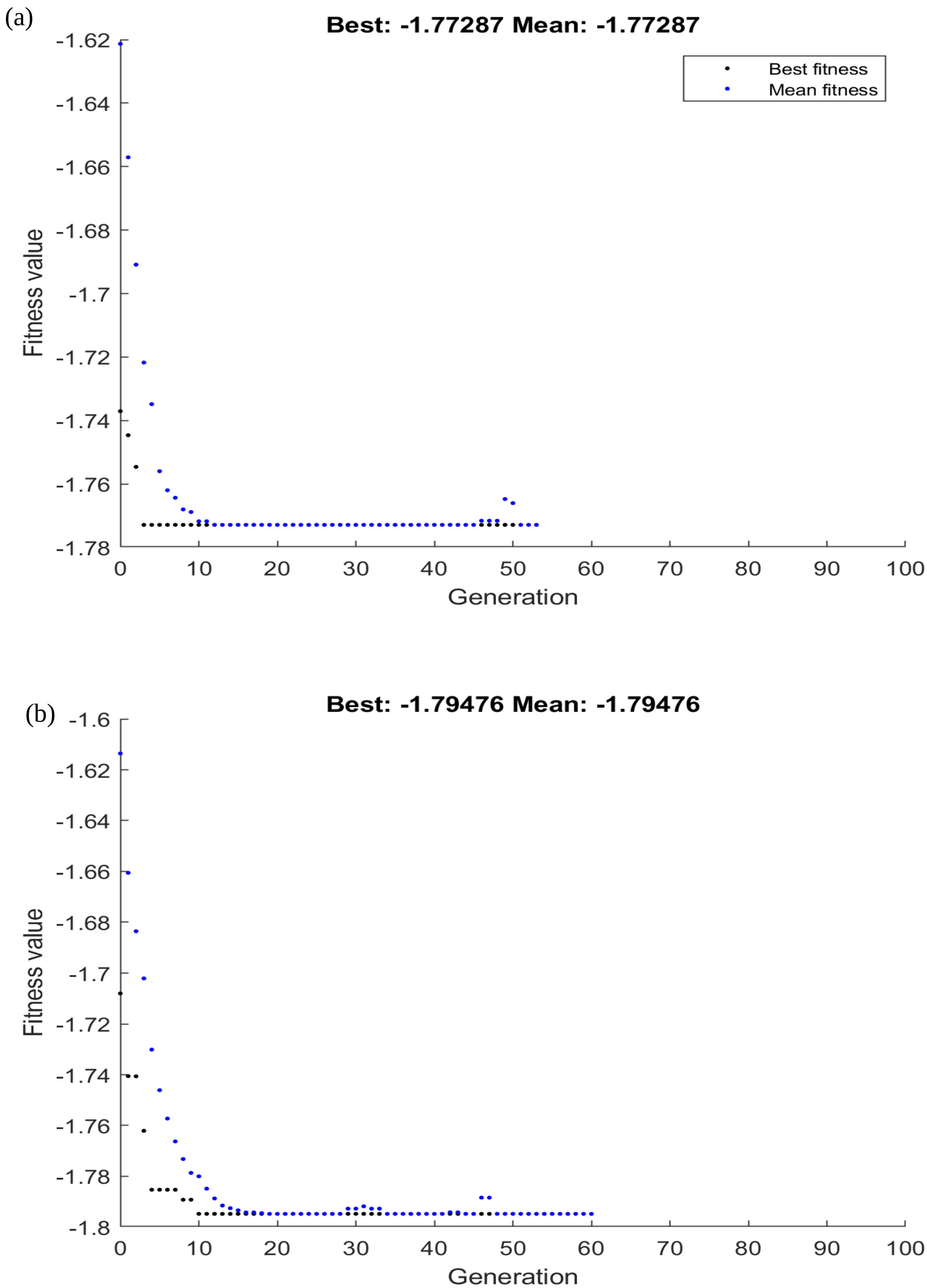

Figure 25: Optimization history with generation for (a) Roughing, (b) Finishing.

For including MRR into the GRA, the data obtained from the experiments have been normalized. The grey coefficients are found by calculating the deviation, and then using equation ((3. 6), the new grey relational grades are calculated. The weighting factors used in the GRA are same as the GA optimization weighting factors.

Table 17: Data preprocessing for four output characteristics including MRR.

Run	Tool life $\delta_{Oi}(1)$	F_Y $\delta_{Oi}(2)$	Ra $\delta_{Oi}(3)$	MRR $\delta_{Oi}(4)$
1	1.000	1.000	0.865	0.000
2	0.508	0.722	0.617	0.417
3	0.290	0.226	0.000	0.937
4	0.589	0.783	0.801	0.333
5	0.081	0.214	0.553	0.872
6	0.280	0.672	0.482	0.453
7	0.042	0.330	0.759	0.729
8	0.181	0.694	1.000	0.391
9	0.000	0.000	0.553	1.000

Table 18. Grey relational Co-efficient.

Run	Tool life $\Phi(1)$	F_Y $\Phi(2)$	Ra $\Phi(3)$	MRR $\Phi(4)$
1	1.000	1.000	0.788	0.333
2	0.504	0.643	0.566	0.462
3	0.413	0.392	0.333	0.889
4	0.549	0.697	0.716	0.429
5	0.352	0.389	0.528	0.797
6	0.410	0.604	0.491	0.478
7	0.343	0.427	0.675	0.649
8	0.379	0.621	1.000	0.451
9	0.333	0.333	0.528	1.000

For roughing, weighting factors are different from those of finishing.

Table 19. Different weighting factors for roughing and finishing.

Weighting factors	Tool life, n	F_Y	Ra	MRR
Roughing	0.3	0.1	0.1	0.5
Finishing	0.2	0.1	0.6	0.1

Table 20. Grey relational grades for roughing and finishing in face milling.

Run	GRG roughing	GRG finishing
1	0.645	0.806
2	0.503	0.551
3	0.641	0.411
4	0.520	0.652
5	0.596	0.506
6	0.471	0.485
7	0.537	0.581
8	0.501	0.783
9	0.686	0.517

Table 21: Results obtained for roughing.

Level	Cutting Speed	Feed	Radial depth of cut
1	0.596	0.568	0.539
2	0.529	0.533	0.570
3	0.575	0.599	0.591

Table 22: Results obtained for finishing.

Level	Cutting Speed	Feed	Radial depth of cut
1	0.589	0.680	0.691
2	0.548	0.613	0.573
3	0.627	0.471	0.499

Table 21 shows that for roughing, the input parameters should be 50 m/min cutting speed, .3 mm/rev feed rate, and 12.5 mm depth of cut. On the other hand, Table 22 demonstrates that for finishing 65 m/min cutting speed, .2 mm/rev feed rate, and 7.5 mm radial depth of cut should be used as input parameters. The results obtained from the GA and GRA are compared in Table 23.

Table 23: The optimum values of the machining of Ti6Al4V obtained from different optimization processes.

Input Parameters	Roughing			Finishing		
	GA results	Grey relational analysis results	Deviation (%)	GA results	Grey relational analysis results	Deviation (%)
Cutting speed (m/min)	50	50	0	64.436	65	.867
Feed rate (mm/rev)	.289	.3	3.67	.205	.2	2.44
Radial depth of cut (mm)	12.473	12.5	.216	7.584	7.5	1.107

The validation experiment, done earlier with the parameters obtained from Ra optimization, is the same as the input parameters obtained from finishing face milling optimization with GRA and using GA. The results obtained from the confirmation experiment has shown a 31.29% improvement in Ra from the initial condition.

On the other hand, for obtaining higher MRR in roughing operation, the results indicate to use 50 m/min cutting speed, 0.3 mm/rev feed rate, and 12.5 mm radial depth of cut. The experiment, conducted following the Taguchi orthogonal array, the third experiment is done following the resultant parameters, and a higher MRR with a reasonable tool life is obtained. The results are shown in Table 5.

CHAPTER V

CONCLUSIONS

For Ti6Al4V alloy, the impacts of various face milling parameters, namely, cutting speed, feed rate, and radial depth of cut on cutting force, Ra, tool life, and MRR have been investigated using the Taguchi, ANOVA, GRA, and GA for mono and multi-objective optimization, respectively. ANOVA analysis has been performed to determine the significance of the input parameters on the response characteristics, and mathematical models have been developed using regression analysis for the prediction of response characteristics.

From S/N ratio analysis, it is found that the optimal parameter setting for maximizing tool life during face milling of Ti6Al4V alloy is cutting speed 50 m/min, feed rate 0.2 mm/rev, and radial depth of cut 7.5 mm. For minimum Ra, the optimal parameters are cutting speed 65 mm/min, feed rate 0.2 mm/rev, and radial depth of cut 7.5 mm. The optimal cutting parameters for minimum Avg. F_X, are cutting speed 57.5 m/min, feed rate 0.2 mm/rev, and radial depth of cut 7.5 mm. For minimum Avg. F_Y, the optimal cutting parameters are cutting speed 50 m/min, feed rate 0.2 mm/rev, and radial depth of cut 7.5 mm. From ANOVA analysis, it is found that the most significant parameter for tool life is cutting speed. For Ra and Avg. F_X, the most significant parameter is feed rate and for Avg. F_Y, and MRR, radial depth of cut is found the most significant one. The mathematical models, developed using regression analysis, have been validated by conducting a validation experiment. It is concluded that the models can be used to closely predict the tool life, Ra, cutting forces, and MRR.

From multi-objective optimization (maximizing tool life, minimizing Ra, and Avg. F_Y) using GRA, the optimal combination of input parameters is cutting speed 50 m/min, feed rate 0.2 mm/rev, radial depth of cut 7.5 mm. The most significant factor using GRA is radial depth of cut for three objectives. The grey relation grade obtained at the optimal setting has shown an improvement of 0.275 compared to the initial condition. Therefore, it can be concluded from this study that radial depth of cut should be considered as a significant factor for face milling of Ti6Al4V.

Multi-objective optimization, considering four objectives (tool life, Ra, Avg. F_Y, and MRR) using GRA and GA for both roughing and finishing, have shown similar results with a negligible deviation, and the experimental results validate the optimization results too.

REFERENCES

1. Izamshah, R., et al., Experimental study of milling titanium alloy (TI-6A1-4V) for defence application. Journal of Fundamental and Applied Sciences, 2017. 9(3S): p. 245-256.
2. Ezugwu, E., Key improvements in the machining of difficult-to-cut aerospace superalloys. International Journal of Machine Tools and Manufacture, 2005. 45(12-13): p. 1353-1367.
3. Kilickap, E., A. Yardimeden, and Y.H. Çelik, Mathematical modelling and optimization of cutting force, tool wear and surface roughness by using artificial neural network and response surface methodology in milling of Ti-6242S. Applied Sciences, 2017. 7(10): p. 1064.
4. Liu, S. and Y.C. Shin, Additive manufacturing of Ti6Al4V alloy: A review. Materials & Design, 2019. 164: p. 107552.
5. Emmelmann, C., et al., Laser additive manufacturing and bionics: redefining lightweight design. Physics Procedia, 2011. 12: p. 364-368.
6. Singh, P., H. Pungotra, and N.S. Kalsi, On the characteristics of titanium alloys for the aircraft applications. Materials today: proceedings, 2017. 4(8): p. 8971-8982.
7. Uhlmann, E., et al., Additive manufacturing of titanium alloy for aircraft components. Procedia Cirp, 2015. 35: p. 55-60.
8. Waterman, N.A. and P. Dickens, Rapid product development in the USA, Europe and Japan. World Class Design to Manufacture, 1994.

9. Semiatin, S., V. Seetharaman, and I. Weiss, The thermomechanical processing of alpha/beta titanium alloys. Jom, 1997. 49(6): p. 33-39.

10. Izamshah RA, R., J. Mo, and S.L. Ding. Finite element analysis of machining thin-wall parts. in Key Engineering Materials. 2011. Trans Tech Publ.

11. Veiga, C., J. Davim, and A. Loureiro, Review on machinability of titanium alloys: the process perspective. Rev. Adv. Mater. Sci, 2013. 34(2): p. 148-164.

12. Izamshah, R., et al. Effects of cutter geometrical feature on machining polyetheretherketone (PEEK) engineering plastic. in 2nd International Conference on Mechanical Engineering Research. Pahang, Malaysia, paper. 2012.

13. Reddy, S.R. and R.R.K. Reddy, Cutting Strategies for Casting Die Manufacturing on CNC Milling Machine. IOSR Journal of Mechanical and Civil Engineering, 2013. 7(4): p. 15-23.

14. Ding, S.L., et al. Chatter detection in high speed machining of titanium alloys. in Key Engineering Materials. 2011. Trans Tech Publ.

15. Khanna, N. and J. Davim, Design-of-experiments application in machining titanium alloys for aerospace structural components. Measurement, 2015. 61: p. 280-290.

16. Kuljanic, E., et al., Milling titanium compressor blades with PCD cutter. CIRP Annals, 1998. 47(1): p. 61-64.

17. Budak, E. and L. Kops, Improving productivity and part quality in milling of titanium based impellers by chatter suppression and force control. CIRP Annals, 2000. 49(1): p. 31-36.

18. Ezugwu, E., J. Bonney, and Y. Yamane, An overview of the machinability of aeroengine alloys. Journal of materials processing technology, 2003. 134(2): p. 233-253.

19. Shaw, M., Metal cutting principles. Clarendon. 1984, Oxford.

20. Abele, E. and B. Fröhlich, High speed milling of titanium alloys. Advances in Production Engineering & Management, 2008. 3(3): p. 131-140.

21. Freeman, R.M. 1974, University of Birmingham. UK.

22. Zlatin, N. and J. Christopher, Technical paper of Society Manufacturing Engineering. Michigan, MR73-909, 1973. 15.

23. Dearnley, P., Wear mechanisms of cemented carbides and ceramics used for machining titanium alloys. High Tech Ceramics, 1986: p. 2699-2712.

24. Walter, J.L., D.W. Skelly, and W.P. Minnear, Ion implantation of cobalt-tungsten carbide tools for machining titanium. Wear, 1993. 170(1): p. 79-92.

25. Dearnley, P. and A. Grearson, Evaluation of principal wear mechanisms of cemented carbides and ceramics used for machining titanium alloy IMI 318. Materials science and technology, 1986. 2(1): p. 47-58.

26. Konig, W. and K. Schroder, th Meeting of AGARD Structural and Materials panel. 1978, Florence.

27. Hartung, P.D., B. Kramer, and B. Von Turkovich, Tool wear in titanium machining. CIRP Annals, 1982. 31(1): p. 75-80.

28. Katayama, S. and T. Imai, Effects of Tool Materials on Tool Damage When Machining Titanium Alloys. Trans. Iron Steel Inst. Jpn., 1986. 26(10).

29. Ezugwu, E. and Z. Wang, Titanium alloys and their machinability—a review. Journal of materials processing technology, 1997. 68(3): p. 262-274.

30. Chandler, H.E., Metals Handbook. 1978.

31. Eckstein, V., G. Lebküchner, and D. Blum, Schaftfräsen von Titanlegierungen mit hohen Schnittgeschwindigkeiten. VDI-Z, 1992. 134(6): p. 61-67.

32. Ezugwu, E., et al., Evaluation of the performance of CBN tools when turning Ti–6Al–4V alloy with high pressure coolant supplies. International Journal of Machine Tools and Manufacture, 2005. 45(9): p. 1009-1014.

33. Ezugwu, E.O., et al., Surface integrity of finished turned Ti–6Al–4V alloy with PCD tools using conventional and high pressure coolant supplies. International Journal of Machine Tools and Manufacture, 2007. 47(6): p. 884-891.

34. Klocke, F. and G. Eisenblätter, Dry cutting. Cirp Annals, 1997. 46(2): p. 519-526.

35. Li, M., et al., Parameter optimization during minimum quantity lubrication milling of TC4 alloy with graphene-dispersed vegetable-oil-based cutting fluid. Journal of cleaner production, 2019. 209: p. 1508-1522.

36. Thakur, A. and S. Gangopadhyay, Dry machining of nickel-based super alloy as a sustainable alternative using TiN/TiAlN coated tool. Journal of cleaner production, 2016. 129: p. 256-268.

37. Islam, M.N., et al., Effect of cooling methods on dimensional accuracy and surface finish of a turned titanium part. The International Journal of Advanced Manufacturing Technology, 2013. 69(9-12): p. 2711-2722.

38. Sharma, V.S., G. Singh, and K. Sørby, A review on minimum quantity lubrication for machining processes. Materials and manufacturing processes, 2015. 30(8): p. 935-953.

39. Nath, C., et al., Effect of fluid concentration in titanium machining with an atomization-based cutting fluid (ACF) spray system. Journal of Manufacturing Processes, 2013. 15(4): p. 419-425.

40. Andriya, N., P.V. Rao, and S. Ghosh. Dry machining of Ti-6Al-4V using PVD coated TiAlN tools. in Proceedings of the World Congress on Engineering, WCE. 2012.
41. Sun, S., M. Brandt, and J.P. Mo, Evolution of tool wear and its effect on cutting forces during dry machining of Ti-6Al-4V alloy. Proceedings of the Institution of Mechanical Engineers, Part B: Journal of Engineering Manufacture, 2014. 228(2): p. 191-202.
42. Tsai, Y.-H., J.C. Chen, and S.-J. Lou, An in-process surface recognition system based on neural networks in end milling cutting operations. International Journal of Machine Tools and Manufacture, 1999. 39(4): p. 583-605.
43. Peace, G.S., Taguchi Methods: a Handson Approach. Addisson Wesley, 1992.
44. Taguchi, G., E.A. Elsayed, and T.C. Hsiang, Quality engineering in production systems. 1989: McGraw-Hill College.
45. Fuh, K.-H. and C.-F. Wu, A proposed statistical model for surface quality prediction in end-milling of Al alloy. International Journal of Machine Tools and Manufacture, 1995. 8(35): p. 1187-1200.
46. Bouzid, W., A. Zghal, and L. Sai, Taguchi Method For Design Optimisation of Milled Surface Roughness. Materials Technology, 2004. 19(3): p. 159-162.
47. Chichili, D., K. Ramesh, and K. Hemker, The high-strain-rate response of alpha-titanium: experiments, deformation mechanisms and modeling. Acta materialia, 1998. 46(3): p. 1025-1043.
48. Chiappini, E., et al., On the mechanics of chip formation in Ti–6Al–4V turning with spindle speed variation. International Journal of Machine Tools and Manufacture, 2014. 77: p. 16-26.

49. Ginting, A. and M. Nouari, Experimental and numerical studies on the performance of alloyed carbide tool in dry milling of aerospace material. International Journal of Machine Tools and Manufacture, 2006. 46(7-8): p. 758-768.

50. Benardos, P. and G.-C. Vosniakos, Predicting surface roughness in machining: a review. International journal of machine tools and manufacture, 2003. 43(8): p. 833-844.

51. Boston, O. and C. Kraus, Elements of milling. Trans ASME, 1932. 54: p. 74-104.

52. Merchant, M.E., Basic mechanics of the metal-cutting process. ASME J. of Applied Mechanics, 1944. 11: p. A168.

53. Feng, H.-Y. and C.-H. Menq, The prediction of cutting forces in the ball-end milling process—I. Model formulation and model building procedure. International Journal of Machine Tools and Manufacture, 1994. 34(5): p. 697-710.

54. Zhang, Z., et al., A study on calibration of coefficients in end milling forces model. The International Journal of Advanced Manufacturing Technology, 2005. 25(7-8): p. 652-662.

55. DeVor, R. A mechanistic model for the force system in end milling with applications to machining airframe structures. in Proceedings of the Eighth North American Manufacturing Research Conference; 1980. 1980.

56. Yang, M. and H. Park, The prediction of cutting force in ball-end milling. International Journal of Machine Tools and Manufacture, 1991. 31(1): p. 45-54.

57. Budak, E., Y. Altintas, and E. Armarego, Prediction of milling force coefficients from orthogonal cutting data. 1996.

58. Engin, S. and Y. Altintas, Mechanics and dynamics of general milling cutters.: Part I: helical end mills. International journal of machine tools and manufacture, 2001. 41(15): p. 2195-2212.

59. Lee, P. and Y. Altintaş, Prediction of ball-end milling forces from orthogonal cutting data. International Journal of Machine Tools and Manufacture, 1996. 36(9): p. 1059-1072.

60. Martellotti, M., An analysis of the milling process. Trans ASME, 1941. 63: p. 677.

61. Tlusty, J., Dynamics of cutting forces in end milling. Annals of CIRP, 1975. 24(1): p. 22-25.

62. Usui, E., A. Hirota, and M. Masuko, Analytical prediction of three dimensional cutting process—Part 1: basic cutting model and energy approach. 1978.

63. Fu, H.-J., R. DeVor, and S.G. Kapoor, A mechanistic model for the prediction of the force system in face milling operations. 1984.

64. Young, H.-T., P. Mathew, and P. Oxley, Predicting cutting forces in face milling. International Journal of Machine Tools and Manufacture, 1994. 34(6): p. 771-783.

65. Kim, H. and K. Ehmann, A cutting force model for face milling operations. International Journal of Machine Tools and Manufacture, 1993. 33(5): p. 651-673.

66. Adolfsson, C. and J.-E. Ståhl, Cutting force model for multi-toothed cutting processes and force measuring equipment for face milling. International Journal of Machine Tools and Manufacture, 1995. 35(12): p. 1715-1728.

67. Zheng, H., et al., Theoretical modelling and simulation of cutting forces in face milling with cutter runout. International Journal of Machine Tools and Manufacture, 1999. 39(12): p. 2003-2018.

68. Li, H. and X. Li, Milling force prediction using a dynamic shear length model. International Journal of Machine Tools and Manufacture, 2002. 42(2): p. 277-286.

69. Altintas, Y. and I. Yellowley, In-process detection of tool failure in milling using cutting force models. 1989.

70. Elbestawi, M., T. Papazafiriou, and R. Du, In-process monitoring of tool wear in milling using cutting force signature. International Journal of Machine Tools and Manufacture, 1991. 31(1): p. 55-73.

71. Sutherland, J. and R.E. Devor, An improved method for cutting force and surface error prediction in flexible end milling systems. 1986.

72. Elbestawi, M., F. Ismail, and K. Yuen, Surface topography characterization in finish milling. International Journal of Machine Tools and Manufacture, 1994. 34(2): p. 245-255.

73. Baek, D.K., T.J. Ko, and H.S. Kim, Optimization of feedrate in a face milling operation using a surface roughness model. International journal of machine tools and manufacture, 2001. 41(3): p. 451-462.

74. Fuh, K.-H. and H.-Y. Chang, An accuracy model for the peripheral milling of aluminum alloys using response surface design. Journal of Materials Processing Technology, 1997. 72(1): p. 42-47.

75. Brezocnik, M., M. Kovacic, and M. Ficko, Prediction of surface roughness with genetic programming. Journal of materials processing technology, 2004. 157: p. 28-36.

76. Escamilla, I., et al. A comparison between back propagation and the maximum sensibility neural network to surface roughness prediction in machining of titanium (ti 6al 4v) alloy. in Mexican International Conference on Artificial Intelligence. 2008. Springer.

77. Suresh, P., P.V. Rao, and S. Deshmukh, A genetic algorithmic approach for optimization of surface roughness prediction model. International Journal of Machine Tools and Manufacture, 2002. 42(6): p. 675-680.

78. Reddy, B.S., J.S. Kumar, and K.V.K. Reddy, Prediction of surface roughness in turning using adaptive neuro-fuzzy inference system. Jordan Journal of Mechanical and Industrial Engineering, 2009. 3(4): p. 252-259.

79. Myers, R. and D. Montgomery, Response Surface Methodology: Process and Product Optimization Using Designed Experiments, Wiley, New York, 1995, pp. 650, 651.

80. Ross, P.J. and P.J. Ross, Taguchi techniques for quality engineering: loss function, orthogonal experiments, parameter and tolerance design. 1988: McGraw-Hill New York.

81. Bermingham, M., et al., Tool life and wear mechanisms in laser assisted milling Ti–6Al–4V. Wear, 2015. 322: p. 151-163.

82. Niknam, S.A., R. Khettabi, and V. Songmene, Machinability and machining of titanium alloys: a review, in Machining of titanium alloys. 2014, Springer. p. 1-30.

83. Tsourveloudis, N.C., Predictive modeling of the Ti6Al4V alloy surface roughness. Journal of Intelligent & Robotic Systems, 2010. 60(3-4): p. 513-530.

84. Taylor, F.W., On the art of metal cutting. Trans. ASME, 1907. 28: p. 31-35.

85. Cook, N.H., Tool wear and tool life. 1973.

86. Hoffman, E.G., Fundamentals of tool design. 1984.

87. Lou, M.S., J.C. Chen, and C.M. Li, Surface roughness prediction technique for CNC end-milling. 1999.

88. Jawahir, I.S., et al., Method of assessing tool-life in grooved tools. 1997, Google Patents.

89. Teitenberg, T.M., A.E. Bayoumi, and G. Yucesan, Tool wear modeling through an analytic mechanistic model of milling processes. Wear, 1992. 154(2): p. 287-304.

90. Alauddin, M., M. El Baradie, and M. Hashmi, Tool-life testing in the end milling of Inconel 718. Journal of materials processing technology, 1995. 55(3-4): p. 321-330.

91. Saini, A., et al., Multi-process parameter optimization in face milling of Ti6Al4V alloy using response surface methodology. Proceedings of the Institution of Mechanical Engineers, Part B: Journal of Engineering Manufacture, 2018. 232(9): p. 1590-1602.

92. Vijay, S. and V. Krishnaraj, Machining parameters optimization in end milling of Ti-6Al-4 V. Procedia Engineering, 2013. 64: p. 1079-1088.

93. Hassan, A. and Y. Zhen-qiang, Multi-objective optimization in the milling of titanium alloys using the MQL technique. Journal of Wuhan University of Technology-Mater. Sci. Ed., 2004. 19(4): p. 26-29.

94. Kuram, E. and B. Ozcelik, Optimization of machining parameters during micro-milling of Ti6Al4V titanium alloy and Inconel 718 materials using Taguchi method. Proceedings of the Institution of Mechanical Engineers, Part B: Journal of Engineering Manufacture, 2017. 231(2): p. 228-242.

95. Julong, D., Introduction to grey system theory. The Journal of grey system, 1989. 1(1): p. 1-24.

96. Aslantas, K., E. Ekici, and A. Cicek, Optimization of process parameters for micro milling of Ti-6Al-4V alloy using Taguchi-based gray relational analysis. Measurement, 2018. 128: p. 419-427.

97. Du, S., et al., Optimization of process parameters in the high-speed milling of titanium alloy TB17 for surface integrity by the Taguchi-Grey relational analysis method. Advances in Mechanical Engineering, 2016. 8(10): p. 1687814016671442.

98. Sarıkaya, M., V. Yılmaz, and H. Dilipak, Modeling and multi-response optimization of milling characteristics based on Taguchi and gray relational analysis. Proceedings of the

Institution of Mechanical Engineers, Part B: Journal of Engineering Manufacture, 2016. 230(6): p. 1049-1065.

99. Polini, W. and S. Turchetta, Cutting force, tool life and surface integrity in milling of titanium alloy Ti-6Al-4V with coated carbide tools. Proceedings of the Institution of Mechanical Engineers, Part B: Journal of Engineering Manufacture, 2016. 230(4): p. 694-700.

100. SECO, Inserts.

101. Zhang, S. and W. Zhu, TiN coating of tool steels: a review. Journal of Materials Processing Technology, 1993. 39(1-2): p. 165-177.

102. Coatings, P. TiAlN Coating - Applications. Available from: https://www.pvd-coatings.co.uk/coatings/ceramic-coatings/tialn-coating/.

103. Hasani, H., S.A. Tabatabaei, and G. Amiri, Grey relational analysis to determine the optimum process parameters for open-end spinning yarns. Journal of Engineered Fibers and Fabrics, 2012. 7(2): p. 155892501200700212.

104. Lin, C., Use of the Taguchi method and grey relational analysis to optimize turning operations with multiple performance characteristics. Materials and manufacturing processes, 2004. 19(2): p. 209-220.

105. Kuriakose, S. and M. Shunmugam, Multi-objective optimization of wire-electro discharge machining process by non-dominated sorting genetic algorithm. Journal of materials processing technology, 2005. 170(1-2): p. 133-141.

106. Derakhshan, E. and A. Akbari. Experimental investigation on the effect of workpiece hardness and cutting speed on surface roughness in hard turning with CBN tools. in Proceedings of the world congress on engineering. 2009.

107. Sharif, S., A. Jawaid, and S. Koksal, Effect of Edge Geometry on Coated Carbide Tools when Face Milling Titanium Alloy. Internatioanl Journal for Manufacturing Science and Technology, 2000. 2(2): p. 11-17.

108. Li, A., et al., Progressive tool failure in high-speed dry milling of Ti-6Al-4V alloy with coated carbide tools. The International Journal of Advanced Manufacturing Technology, 2012. 58(5-8): p. 465-478.

109. Ehsan, S., et al., Milling of Ti-6Al-4V alloy using hybrid geometry tooling. The International Journal of Advanced Manufacturing Technology, 2019. 105(12): p. 5045-5059.

110. Park, J., et al., Evaluation of machinability in the micro end milling of printed circuit boards. Proceedings of the Institution of Mechanical Engineers, Part B: Journal of Engineering Manufacture, 2009. 223(11): p. 1465-1474.

BIOGRAPHICAL SKETCH

Al Mazedur Rahman has acquired his bachelor's degree in Mechanical engineering from Khulna University of Engineering and Technology in 2017 and joined the department of Manufacturing and Industrial Engineering at the University of Texas Rio Grande Valley in 2019 for pursuing a Master's. He worked as a research assistant at the Advanced machining lab under Dr. Anil K. Srivastava and completed his Master of Science in Manufacturing Engineering in December 2020. His research interests are focused on advanced machining, additive manufacturing, and high entropy alloys. During his Master's, he was awarded the Presidential Graduate Research Assistantship award for all two years. He has submitted one article in a prestigious journal, one poster presentation, and is on the verge of submitting another article. For pursuing a Ph.D. degree, he is expected to join the Texas A&M University, College Station in the Industrial and Systems Engineering department. He can be reached at almazedurrahman@gmail.com.